12502–12522 *Nucleic Acids Research, 2020, Vol. 48, No. 22* *Published online 2 December 2020*
doi: 10.1093/nar/gkaa1116

SURVEY AND SUMMARY

Translational control of coronaviruses

Sylvain de Breyne*, Caroline Vindry, Olivia Guillin, Lionel Condé, Fabrice Mure, Henri Gruffat, Laurent Chavatte and Théophile Ohlmann*

CIRI, Centre International de Recherche en Infectiologie, Univ Lyon, INSERM U1111, Université Claude Bernard Lyon 1, CNRS UMR5308, ENS de Lyon, F-69007, Lyon, France

Received October 02, 2020; Revised October 29, 2020; Editorial Decision October 30, 2020; Accepted November 03, 2020

ABSTRACT

Coronaviruses represent a large family of enveloped RNA viruses that infect a large spectrum of animals. In humans, the severe acute respiratory syndrome coronavirus type 2 (SARS-CoV-2) is responsible for the current COVID-19 pandemic and is genetically related to SARS-CoV and Middle East respiratory syndrome-related coronavirus (MERS-CoV), which caused outbreaks in 2002 and 2012, respectively. All viruses described to date entirely rely on the protein synthesis machinery of the host cells to produce proteins required for their replication and spread. As such, virus often need to control the cellular translational apparatus to avoid the first line of the cellular defense intended to limit the viral propagation. Thus, coronaviruses have developed remarkable strategies to hijack the host translational machinery in order to favor viral protein production. In this review, we will describe some of these strategies and will highlight the role of viral proteins and RNAs in this process.

INTRODUCTION

Coronaviruses: an overview

Coronaviruses (CoVs) represent a large family of RNA enveloped viruses that contain a positive-sense and single-stranded RNA genome that is one of the largest of all RNA viruses. CoVs are usually associated with enteric or respiratory diseases in their hosts, although hepatic, neurologic and other organ systems may be affected. The current classification of coronaviruses recognizes 46 species in 26 subgenera, 5 genera and 2 subfamilies that belong to the family *Coronaviridae*, suborder *Cornidovirineae*, order *Nidovirales* and realm *Riboviria* (1). The *Orthocoronavirinae* subfamily can be divided into four genera: α- and β-CoV that only infect mammals, δ- and γ-CoV that mainly target birds. In the late 1960s, the first human coronaviruses (HCoV) were identified (HCoV-229E, HCoV-814 and HCoV-OC43) and also later in the 2000s (HCoV-NL63 and HCoV-HKU1) (2–6); these strains generally cause mild symptoms such as a common cold. In contrast, severe acute respiratory syndrome coronavirus (SARS-CoV) (7–9) and Middle East Respiratory Syndrome coronavirus (MERS-CoV) (10–12) that emerged in 2002 and 2012, respectively, are highly pathogenic coronaviruses. The SARS-CoV-2 is currently at the origin of the COVID-19 pandemic that the world is going through with, as of 10 October 2020, >34 million confirmed cases resulting in >1 million deaths (13). The SARS-CoV-2 genome share 80% and 50% homology with SARS-CoV and MERS-CoV genomes respectively (14–16) and all of them belong to the β-CoV genera. This genus also includes animal strains such as the Mouse Hepatitis Virus (MHV) (17) or the Bovine-CoV (B-CoV) (18,19) but also two human strains (HCoV-OC43 and HCoV-HKU1).

Coronavirus infections begin with interaction between virions and their cellular receptors at the surface of the cells (Figure 1). After release of the nucleocapsid into the cytoplasm, the viral genome serves as mRNA for translation to generate the viral replicase. The genomic viral RNA (gRNA) contains >12 open reading frames (ORFs) and even 14 in the case of SARS-CoV-2 to give rise to about 27 proteins (14). In order to express as many as 27 different proteins, coronaviruses have put in place three different mechanisms. First, when the viral genome enters the cytoplasm, the first ORF (ORF1) is translated into a long polyprotein which is then proteolytically processed to generate several nonstructural proteins (nsp). In addition, this polyprotein is generated in two different forms through the use of a programmed-1 ribosome frameshifting event. This mechanism requires a *cis*-acting RNA element within the coding region that can redirect elongating ribosomes to shift back to the first reading frame by 1 base in the 5′ direc-

*To whom correspondence should be addressed. Tel: +33 472 728 893; Fax: +33 472 728 137; Email: sylvain.de.breyne@ens-lyon.fr
Correspondence may also be addressed to Théophile Ohlmann. Tel: +33 472 728 953; Email: theophile.ohlmann@ens-lyon.fr

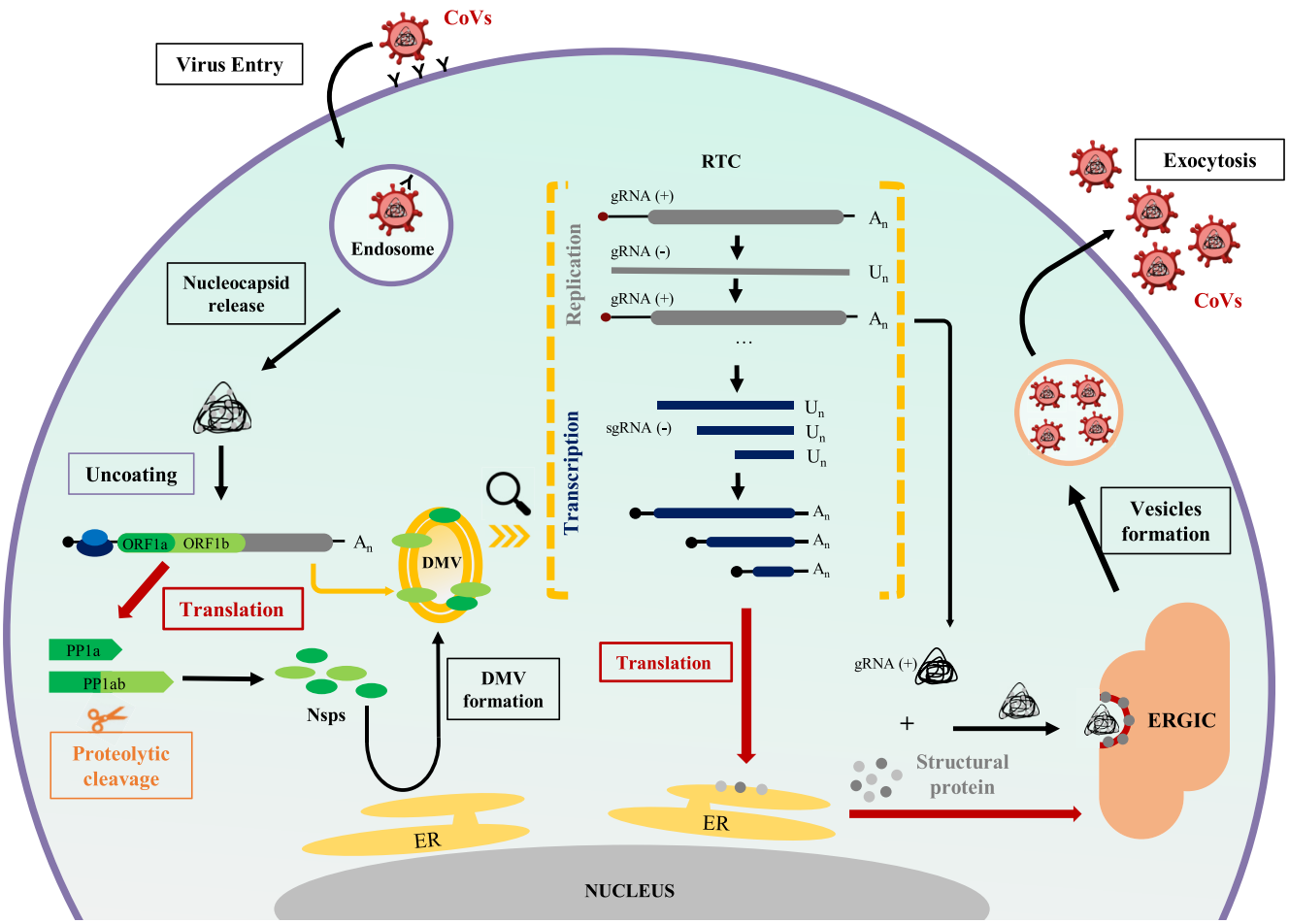

Figure 1. Scheme of the coronaviral replication cycle. After attachment to the cellular receptor, the viral particle is internalized and the gRNA is uncoated and directly translated in the cytoplasm to produce up to 16 nonstructural proteins (nsps) involved in viral proteolytic cleavage, the formation of the viral replication transcription complex (RTC) and in mRNA translational control. Viral genome replication and transcription of the different sgRNAs occur into double membrane vesicles (DMV) that are derived from the endoplasmic reticulum (ER). Some of the sgRNAs are coding for the structural proteins that are mainly expressed through the ER. Viral components (gRNA and viral proteins) assemble at the level of the ERGIC and new virions produced are secreted by exocytosis.

tion. This mechanism was described for the first time in 1985 in the Rous sarcoma virus (20) and 2 years later in the coronavirus Avian Infectious Bronchitis Virus (IBV) (21). All coronaviruses, including SARS-CoV-2, utilize this molecular mechanism (22–27). Therefore, ORF1 is separated into two distinct ORFs: ORF1a and ORF1b. In general, translation of ORF1a allows production of the immediate early proteins involved in the control of the host cellular innate immune response whereas translation of ORF1b generates proteins involved in genome replication and RNA synthesis. The other ORFs, which are expressed later during the viral replication cycle, are translated from distinct subgenomic RNAs (sgRNAs) produced by the synthesis of the minus-strand replicative intermediate, followed by synthesis of new plus-strand sgRNAs that mostly encode structural and accessory proteins. This represents the third strategy used for the translation of the viral ORFs.

Coronavirus RNA synthesis proceeds by a very complex and only partially understood mechanism. The gRNA not only serves as a matrix for the synthesis of the replicase polyproteins but also acts as the template for synthesis of negative-sense RNA species (Figure 1). These negative sense subgenomic RNAs (sgRNAs) are used as template for the generation of the positive-sense sgRNAs that are produced by a discontinuous, cotranscriptional process. Then, each positive-sense sgRNA serves as mRNA for translation of each ORF downstream of ORF1. All the sgRNAs are 3′ coterminal and contain the same ∼70 nucleotides (nt) long 5′-leader. The sites of leader-to-body fusion in the sgRNAs occur at loci in the genome called transcription-regulating sequences (TRSs) that contain a short element that is identical, or nearly identical, to a sequence located at the 5′-end of the gRNA. TRSs contain a conserved 6–7 nt core sequence fairly well conserved within each coronavirus group and surrounded by variable sequences. The viral polymerase, starting from the 3′-end of a genomic RNA, pauses and switches templates at an internal TRS to pursue synthesis at the homologous TRS of the leader gRNA. The resulting negative-strand sgRNA then serves as template for synthesis of multiple copies of the corresponding positive-

strand sgRNAs (28). Transcriptomic analysis of cells infected by coronavirus shows that the majority (>60%) of the reads mapped to viral sequences indicating that viral transcripts become largely predominant over the cellular transcriptome (14). In addition to these viral transcripts, it has been shown that several viral RNAs are produced by different noncanonical recombination events leading to the generation of transcripts harboring different deletions (14,29–31). However, it is not known whether these viral RNAs, which are relatively abundant, can be translated into functional proteins.

One common feature among positive-strand RNA viruses is the assembly of their replication-transcription complexes (RTCs) that is intimately associated with the formation of membranous rearrangements to create virus replication organelle (Figure 1) (32–34). The RTCs are interconnected double membrane vesicles (DMV) that are derived from the endoplasmic reticulum (ER) (35–39). The precise role of these vesicles is not known but they seem to be beneficial to the virus creating a protective microenvironment for the viral genome from attacks by antiviral mechanisms or nucleases present in the cytoplasm; in addition, it provides an environment to concentrate the factors necessary for efficient transcription and replication of the viral genome. As a consequence, formation of infectious progeny virions mainly occurs into the endoplasmic reticulum-golgi intermediate compartment (ERGIC) (Figure 1). After replication, the viral genome is encapsidated by the N protein into the membrane of the ERGIC in which the viral structural proteins are included (40). The viral particles are then released from the cell by a process very similar to exocytosis (Figure 1). Further details on the replication cycle of coronaviruses can be found on these reviews (41–45).

Translation initiation in eukaryotes

Translation is a key step in gene expression in which the messenger RNA (mRNA) is decoded by ribosomes to produce proteins. The eukaryotic mRNA is usually capped at the 5′end and polyadenylated at the 3′ end (Figure 2). The ORF codes for the polypeptide and is surrounded by two untranslated regions (UTRs) that control translation initiation by promoting ribosome attachment to the mRNA and the recognition of the initiation codon (AUG codon). The majority of mRNAs uses the cap-dependent mechanism to initiate translation in which eukaryotic initiation factors (eIFs) recognize and bind to the 5′ cap structure to bridge the mRNA to the 40S ribosomal subunit (Figure 2). This process requires eIF4F that is a three-subunits complex composed of eIF4E, the cap-binding protein; eIF4A, an ATP dependent RNA helicase which belongs to the DEA(D/H)-box family; and eIF4G, a scaffold protein. EIF4G has binding sites for eIF4A, eIF4E, the poly(A) binding protein (PABP) and eIF3. The eIF4F complex recognizes and binds to the 5′ cap structure and unwinds local RNA structures required for adequate positioning of the 40S ribosomal subunit on the mRNA. The 40S ribosomal subunit is recruited to the mRNA as part of the 43S initiation complex that is composed of the 40S ribosome bound to eIF2-GTP/Met-tRNAi (initiator tRNA), eIF1A, eIF1, eIF3 and eIF5 (46–49). In this conformation, eIF4G constitutes a real scaffold between the mRNA with the cap structure through eIF4E, and the 40S ribosomal subunit via eIF3. In eukaryotes, the mRNA is pseudo-circularized by an interaction between eIF4G at the 5′ end and PABP at the 3′ end and this contributes to enhance translational efficiency (50–52). Upon its recruitment to the 5′ end of the mRNA, the 43S ribosomal complex scans the mRNA in a 5′-3′ direction in search of the initiation codon, which is often the first AUG triplet downstream to the 5′cap. During the ribosomal scanning, the GTP bound on eIF2 is hydrolyzed to GDP and phosphate (Pi) in an eIF5-dependent mechanism (53,54). The recognition of the initiation codon by the anticodon of the Met-tRNAi stops the scanning process and provokes Pi and eIFs release from the ribosomal complex that allows the 60S ribosomal to join and form the 80S ribosome positioned at the initiation codon (Figure 2) (55–57). The guanine nucleotide exchange factor eIF2B promotes the recycling of eIF2-bound GDP into eIF2-bound GTP; as a result, the ternary complex reassembles for a new round of translation initiation. eIF2 activity is regulated by phosphorylation event that takes place on the serine 51 of the α-subunit (Figure 2). In mammals, four kinases have been well characterized and are activated by stress conditions such as amino acid deprivation (for the GCN2 kinase), ER stress (for the PERK kinase), the presence of dsRNA (for the PKR kinase) or heme deficiency (for the HRI kinase) (58). During viral infection, PKR and PERK are usually activated resulting in a global translation arrest and the formation of stress granules (SGs) (59–61).

Cis-acting elements can also influence initiation codon recognition rate by the 43S complex. Two of them are the nucleotide context of the AUG codon and the presence of short upstream ORFs (uORFs). An optimal consensus sequence around the initiation codon was defined as 5′-**A/G**cc*AUG***G**-3′ in which positions -3 and +4 according of the adenosine of the AUG codon are determinant for initiation codon recognition (62–65). When the context is not optimal, a fraction of the scanning ribosomes can bypass the AUG codon to go to the next downstream AUG triplet. This is called leaky scanning and it results in the production of two proteins from two different ORFs or two isoforms of the same protein. However, re-initiation of translation can occur if the length of the first ORF is shorter than 30 amino acids (uORF) and if the main ORF is found approximately 100–200 bp downstream of the stop codon (66). In this case, the different eIFs usually stay in the vicinity of the 40S ribosomal subunit to promote re-initiation. As a consequence, uORFs can regulate the flow of ribosomes on the mRNA (67,68), and this usually results in the reduction of translational efficiency of the main reading frame (69).

Examples of translational control during viral infections

Most of the time, viral infection activates the first host defense mechanism that triggers the production of interferons (IFN) and IFN stimulated genes (70). To counteract this first line of host antiviral innate immunity, viruses have developed strategies to inhibit or escape to this restriction (71) and components of the IFN signal transduction pathway are often inactivated during viral infection (72). As such, some RNA viruses, including *Picornaviruses*, *Orthomyx-*

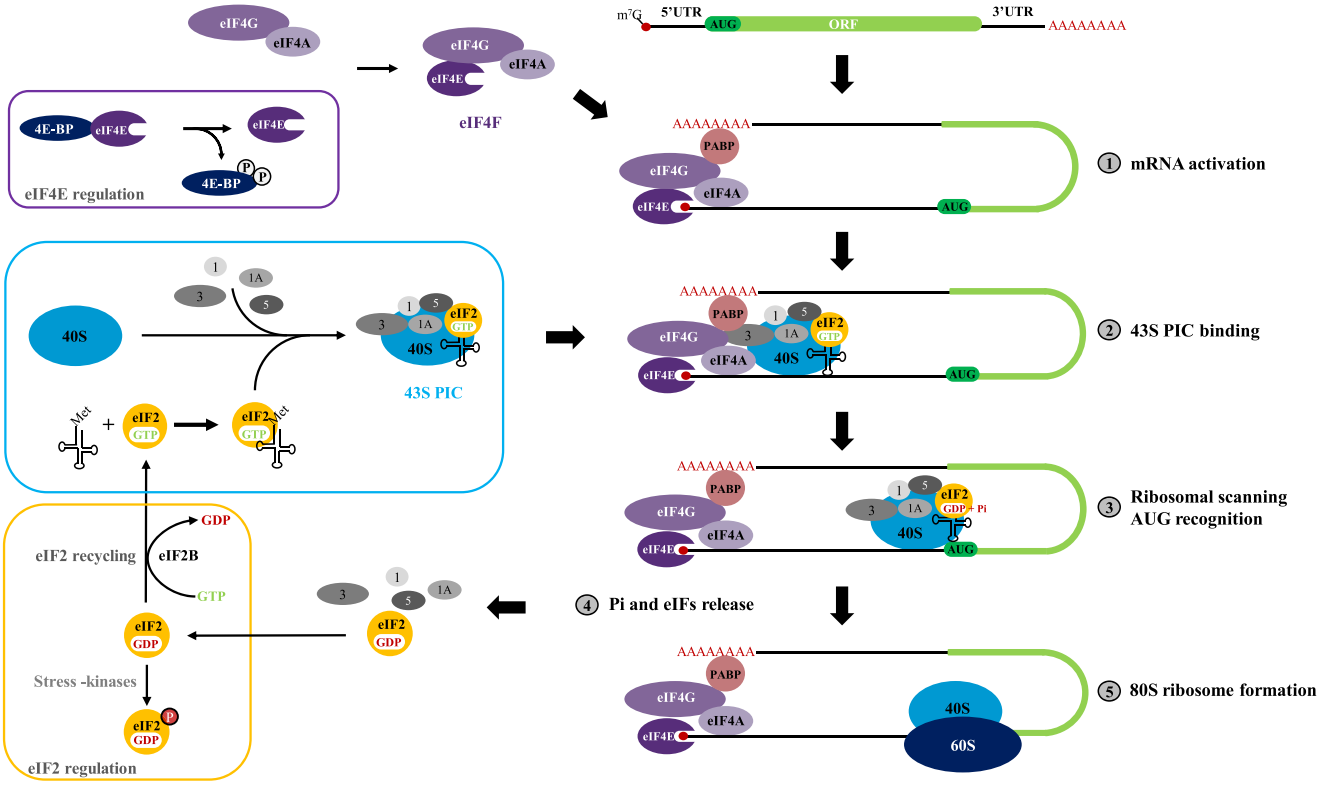

Figure 2. The cap-dependent translation initiation mechanism. (1) Capped and polyadenylated mRNA is activated by the eIF4F complex, composed of eIF4E, eIF4G and eIF4A, to prepare ribosomal landing. 43S ribosomal complex is formed by the association of eIF1, eIF1A, eIF3, eIF5 and the ternary complex eIF2-GTP-Met-tRNAi with the 40S small ribosomal subunit (see blue square). (2) Attachment of the 43S complex to the mRNA is mediated by multiple protein interactions requiring eIF4E, eIF4G and eIF3. (3) Ribosomal complex scans the 5′UTR with the hydrolysis of GTP into GDP + Pi mediated by eIF5 until it reaches the initiation codon, where its recognition triggers to (4) Pi and eIFs release followed by (5) the association of the 60S and 40S ribosomal subunits to form an 80S ribosome competent for the elongation step. The most known translational controls occur on eIF4E and eIF2. According to the phosphorylation state of 4E-BP, 4E-BP interacts or not with eIF4E and this interaction displaces eIF4E from eIF4F resulting in a decrease of the cap dependent translation efficiency (see violet square). Regeneration of the GDP molecule bound to eIF2 into GTP is catalyzed by the exchange factor eIF2B. Phosphorylation of eIF2α at a serine in position 61 inhibits this regeneration that also induces a strong reduction of global translation (see orange square).

oviruses, *Coronaviruses* and many others, combine an additional mechanism in which a host translational shutoff is imposed to prevent the infected cells to synthesize new proteins and, amongst those, the IFN-stimulated genes (73). However, such strategy should not affect the expression of viral mRNAs to allow efficient viral replication to spread and continue. Therefore, most of the time, viruses have developed alternative translation initiation mechanisms to ensure continuous viral protein production.

For instance, during *picornaviruses* infection, epitomized by the encephalomyocarditis virus (EMCV) and the poliovirus (PV), a rapid shutoff of the host gene expression is established when viral proteases target and cleave eIF4G, PABP and eIF5B that are required for cap-dependent translation initiation (74–77). This results in a specific inhibition of cap-dependent translation of cellular mRNAs whereas the 5′UTR of the picornaviral mRNAs harbors an internal ribosome entry site (IRES) that enables the recruitment of the ribosomal complex in a cap-independent manner (78). An alternative strategy is used by influenza virus where the viral polymerase complex binds to cellular mRNAs and cleaves few nucleotides downstream to the cap structure to produce a capped RNA fragment that is subsequently used to prime viral transcription (79,80). The decapped host mRNAs are targeted to degradation that leads to the downregulation of cellular protein production. Finally, translation of the alphavirus mRNAs is resistant to the phosphorylation of eIF2α that results from PKR activation (81). This is due to a stable RNA hairpin loop structure in the viral genome that stalls the ribosome on the correct AUG and allows translation of the late viral mRNAs (82).

Global translation of cellular mRNAs is not spared during infection with CoVs. Indeed, studies in MHV-infected cells indicate that a strong shutoff of host gene expression is established during the first hours after infection while viral protein expression is not affected (83–87). This inhibition of cellular mRNA expression has been reported in cells infected not only with others coronaviral strains such as in bovines, bats, chickens and pigs (88–92) but also with human CoVs like the HCoV-229E, HCoV-NL43, SARS-CoV and MERS-CoV strains (93–96). Recent studies show that translation repression also occurs in SARS-CoV-2 infected cells (97–99) and analysis of the SARS-CoV-2 tran-

scriptome indicates that host gene expression is almost suppressed in the first hours of infection (14). Most of the viral structural proteins are expressed in the ER that contributes to create an ER stress (100). Furthermore, lipid depletion from the ER which is due to viral replication organelle formation activates the unfolded protein response (UPR) that results to the expression of chaperone proteins, phospholipid biogenesis and translation downregulation (101). Nevertheless, the UPR is usually controlled by viral components to avoid a drastic reduction of global protein synthesis. The first analyses of the SARS-CoV-2 host interacting proteins revealed that many viral proteins target components belonging to the translational machinery but also key elements involved in SG formation and the ER stress response (102).

In this review, we will describe how mRNA translation is controlled in the course of coronaviral infection. Most of the studies retained for this review concern SARS-CoV, MERS-CoV and SARS-CoV-2 strains. In the first part, we will briefly present the different translational pathways that are activated following infection and how viral components can interfere. A large part of this review will focus on viral proteins, especially nsp1, which directly interact with components of the ribosomal complex to promote translation inhibition and mRNA decay. The second part is dedicated to the mechanisms used by viral mRNAs to escape from host protein synthesis inhibition. Finally, the last part will deal with the spectrum of translational mechanisms used by viral mRNAs to be expressed.

TRANSLATIONAL CONTROL BY CORONAVIRUSES

Viral infection generally induces several lines of cellular responses such as innate immunity, apoptosis, activation of different mitogen-activated protein kinases (MAPK) pathway or translational reprogramming. As these different mechanisms during CoV infection have been recently reviewed (103), we will first briefly describe how these different translational control pathways are activated during infection and point out some viral proteins involved in these mechanisms. Next, we will mainly focus on viral proteins expressed from SARS-CoV, MERS-CoV and SARS-CoV-2 strains, which directly alter the integrity of components of the initiation complex. A large part of this section deals with nsp1 and its function in host protein synthesis inhibition as it has been the best studied example.

Interference with the stress activated pathways

CoV replication generates in the cytoplasm a large quantity of double strand RNAs such as positive and negative gRNAs and sgRNAs (Figure 1); this typical signature of RNA virus replication contributes to the activation of PKR. In addition, several aspects of the CoV infection are expected to disrupt ER homeostasis. (i) All CoV structural proteins, except for the N protein, are synthesized, folded and modified in the ER (104–106). (ii) In order to produce new virions, the amount of viral proteins produced largely exceeds the ER folding capacity (100,107). (iii) Viral replication takes place in double membrane vesicles complexes hijacked from the ER and this results in the alteration of its homeostasis (Figure 1) (35,108). (iv) The assembly and budding of mature particles of coronaviruses occur into the ERGIC (109) that induces a massive budding accompanied by depletion in the ER membrane (Figure 1). All these different stresses of the ER lead to the activation of the UPR. To restore ER homeostasis, three transmembrane sensors are activated: PERK, inositol-requiring enzyme 1 and activating transcription factor 6. The last two are not directly related to translational control and we invite the reader to consult these reviews (103,110–112), and we will focus on the relationship that may exist between CoVs and both PKR and PERK.

As expected, both PERK and PKR are activated during SARS-CoV infection that in turn phosphorylate the serine 51 of eIF2α leading to a global translation inhibition (Figure 3A) (113). However, inhibition of PKR alone did not alter the phosphorylation status of eIF2α meaning that it is essentially controlled by PERK (113). The activation of PKR seems important for other aspects of viral infection, such as virally induced apoptosis that could contribute to the translational inhibition (113). The overexpression of several SARS-CoV proteins alone, including 3a and S, is sufficient to induce an ER stress and the activation of PERK (Figure 3A) (100,114). Expression of the spike protein from MHV or HCoV-HKU1 strains also induces an ER stress (107,115) suggesting a conserved mechanism of PERK activation among CoVs. Interestingly, the phosphorylation of eIF2α is not such a robust feature for other coronavirus infections as it depends on the cell line used and it can only be a transient phenomenon. For example, infection with MERS-CoV strain induces a low but detectable level of phosphorylated eIF2α only in Vero cells, but no response in HeLa/CD26 cells (116). In addition, the removal of the gene coding for 4a and 4b proteins in the viral genome of the MERS-CoV (Δp4 mutant strain) induces the phosphorylation of eIF2α, activation of PKR and reduces viral replication in HeLa cells suggesting that these proteins are involved in circumventing translational attenuation during infection (Figure 3A). Surprisingly, no difference was observed between MERS-CoVΔp4 and the wild-type virus in Vero cells, suggesting a cell line specific regulation rather than a solid feature of MERS-CoV infection (116). To the same extend, nsp15 of some CoVs (MHV, HCoV-229E) could also suppress PKR activation (Figure 3A) (117–119). Additionally, during HCoV-OC43 infection of neurons, only an early and transient phosphorylation of eIF2α was detected (120). There is no doubt that CoV infection is related to the activation of both PKR and PERK that results in the phosphorylation of eIF2α. Whether the novel SARS-CoV2 also acts on eIF2α phosphorylation to induce a global translation regulation remains to be investigated.

Translational inhibition induced eIF2α phosphorylation leads to the formation of SGs and processing bodies (P-bodies). SGs are messenger ribonucleoproteins (mRNPs) composed of mRNAs stalled at the translation initiation step while P-bodies are mRNPs containing untranslated mRNAs associated with proteins involved in mRNA decay and translation repression. These two cytoplasmic granules are dynamic complexes which compact mRNAs for storage, reinitiation of translation or degradation (121–124).

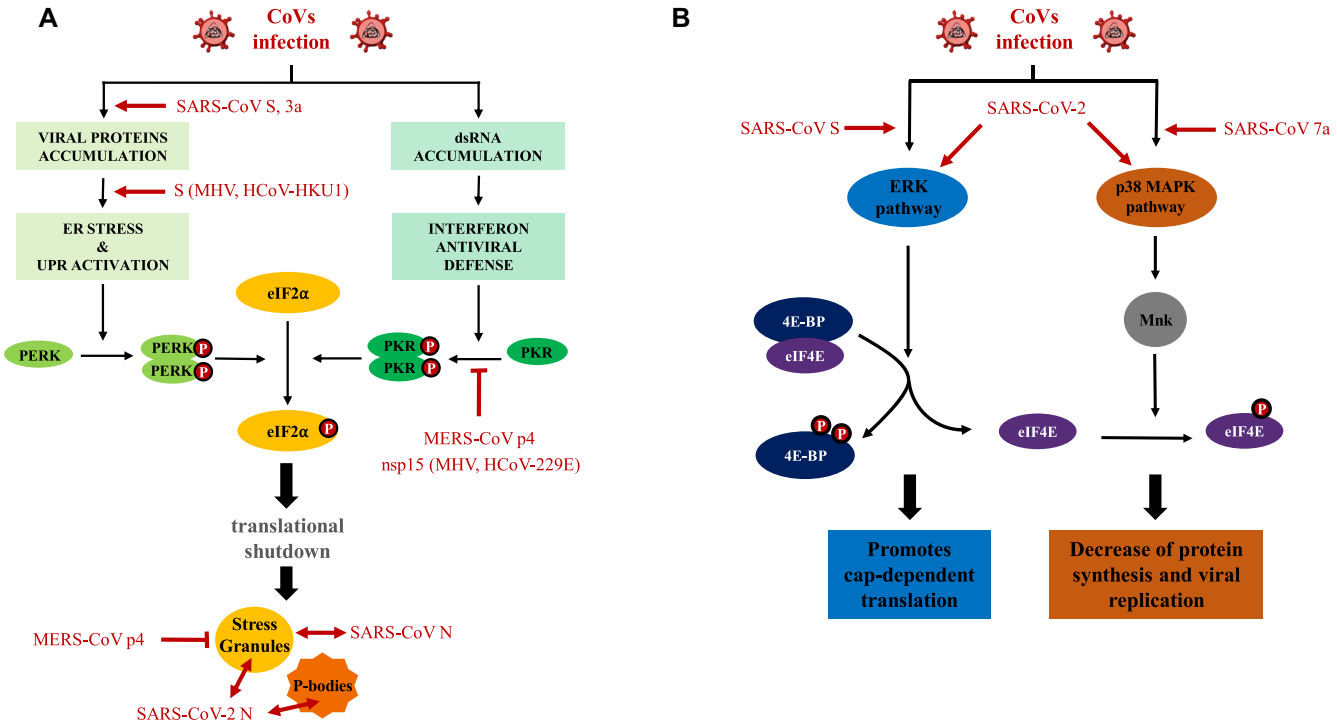

Figure 3. The translational pathways regulation during CoVs infection. (**A**) Double strand RNA (dsRNA) accumulation produced during the viral replication is one sensor of the interferon antiviral defense and leads to the phosphorylation and activation of PKR. Viral proteins accumulation in the endoplasmic reticulum (ER) constitutes an ER stress and triggers the unfold protein response (UPR). As a result, PERK is phosphorylated and activated. Both PKR and PERK target the α subunit of eIF2 and its phosphorylation induces a global translational shutdown. The stress-activated phosphorylation of eIF2 can lead to the formation of stress granules (SGs) in which mRNAs stalled in translation initiation step are stored. SGs are connected with P-bodies structures as they share RNA and protein components. (**B**) Modulation of the p38MAPK and ERK pathways. ERK pathway controlled the phosphorylation state of 4E-BP and promotes the dissociation between 4E-BP and eIF4E that enhances the cap-dependent translation. p38 MAPK pathway targets the MAP kinase-interacting serine/threonine-protein kinase (Mnk) that phosphorylates eIF4E. As a consequence and in the context of CoVs infection, activation of this pathway is associated with a decrease of protein synthesis and viral replication. Viral components modulating the pathway are bolded in red.

The assembly of SGs is a cellular response frequently observed upon viral infections but its real contribution to the anti-viral response remains to be established (125). In many cases, viral mRNAs and/or viral genomes are recruited in SGs (125,126). In the particular case of CoV infection, the function of SG and P-bodies has not been fully investigated although an increase in the formation of cellular granules has been observed during the Transmissible GastroEnteritis Virus (TGEV) and MHV infections which correlate with an increase of eIF2α phosphorylation, translational shutoff and mRNA decay (87,127). During infection with SARS-CoV, the N protein can translocate into SGs (Figure 3A) (128) whereas formation of SGs is not observed in the course of MERS-CoV infection. Nevertheless, mutant viruses lacking either the gene coding for 4a or 4b protein (MERS-CoVΔp4), become able to induce formation of SGs suggesting that these proteins might be involved in their repression (116,119). Notably, the formation of SGs in cells infected with MERS-CoVΔp4 is associated with a reduction of viral replication (Figure 3A). Recently, mass spectrometry analysis of the viral-host proteome interaction networks was obtained with overexpressed viral proteins from SARS-CoV-2. Interestingly, the N protein interacts with several components of the SGs (G3BP1 and G3BP2) and P-bodies (Upf1, MOV10, PABPC1 and PABPC2) machineries (Figure 3A) (102). However, the role of these cytoplasmic granules as pro- or anti-viral mechanism remains elusive.

Coronavirus infections activates other stress-induced signaling pathways such as the extracellular signal-regulated kinase (ERK) and the p38 MAPK, both of them are known to influence the translational activity of the cell (103). Activation of p38 MAPK is observed during SARS-CoV and MHV infections (Figure 3B) and this leads to the phosphorylation of eIF4E through the MAP kinase-interacting serine/threonine-protein kinase (Mnk) (129–131). The effect of this phosphorylation is quite controversial with some articles showing that phosphorylation of eIF4E is not required for translation (132) whereas in some cases, it can inhibit cap-dependent translation (133). Despite this controversy, most of the data suggest that eIF4E phosphorylation promotes translation initiation (134–137). In the case of CoV, activation of the p38 MAPK pathway is associated with an attenuation of overall cellular protein synthesis. Interestingly, expression of the SARS-CoV accessory protein 7a alone can inhibit cellular protein synthesis and induce p38 MAPK phosphorylation (Figure 3B) (138,139). However, molecules that target the p38 MAPK neither alter SARS-CoV replication nor viral protein synthesis (130). Similarly, infection with HCoV-229E also induces the phosphorylation of eIF4E and the use of a p38 MAPK inhibitor in human fetal lung cells L132 reduces the replication of the

virus (140). To date, the implication of eIF4E phosphorylation during CoV infection is challenging and remains to be explored. Finally, inhibitors that control the phosphorylation of eIF4E, such as tomivosertib, have recently been highlighted to be of interest in the case of treatment during SARS-CoV-2 infection (102) and this confirms the importance of the stress-induced signaling pathways.

In parallel, the ERK signaling cascade is activated during CoV infection (Figure 3B) and seems to counterbalance the action of p38 MAPK in protein synthesis. Indeed, activation of ERK leads to the phosphorylation of eIF4E-binding proteins (4E-BP) that are repressor proteins able to interact directly with the cap-binding protein eIF4E. Phospho-4E-BP cannot bind to eIF4E and sequesters it from being incorporated into the eIF4F complex (Figure 2) (141). The activation of the ERK pathway was observed during infection with SARS-CoV, MERS-CoV and HCoV-229E strains (129,142) but also after overexpresion of SARS-CoV S protein (143). In the case of SARS-CoV-2, the investigation of the global phosphorylation landscape of Vero E6 cells reveals the activation of p38 MAPK and ERK pathways, and suggests an impact on cap-dependent translation (144). Clearly, the phosphorylation status of eIF4E and eIF4E-BPs needs further investigation to decipher the role of signaling pathway activation in SARS-CoV2 infection.

The nsp1 protein

The capped and polyadenylated viral genome is directly translated as soon as it is released in the cytoplasm after entry. As a result, two large precursor polyproteins are produced and processed by viral proteases to generate 16 nsps. Nsp1 is the most N-terminal cleavage product and is only expressed in the α-CoVs and β-CoVs genera but it strongly differs in size. Nsp1 of α-CoVs has a size of about 110 amino acids (aa) whereas in β-CoVs the size of nsp1 varies between the four different lineages (A, B, C and D) (145). The lineage A is epitomized by MHV, HCoV-OC43 and HCoV-HKU1, and nsp1 harbors about 245 aa residues. The lineage B includes SARS-CoV and SARS-CoV-2 in which nsp1 has a size of 180 aa. MERS-CoV belongs to the lineage C and encodes a 195 aa long nsp1. Finally, the lineage D regroups mainly bat-CoVs in which nsp1 has a size of 175 aa. Amino acid sequence homology varies between nsp1 from the different β-CoVs but the SARS-CoV-2 nsp1 shares 91% similarities with SARS-CoV nsp1 (102) suggesting a strong conservation of function and the first study on SARS-CoV-2 nsp1 confirmed its role in host protein synthesis inhibition (97–99). In this section, we mainly discuss about the function and mechanism of SARS-CoV nsp1 on host cellular translation during infection and extend these findings to others strains like MERS-CoV and SARS-CoV-2.

SARS-CoV nsp 1. In SARS-CoV infected cells, nsp1 can be immunodetected as early as 6 h post infection (hpi) and it has a perinuclear and cytoplasmic localization (94,146). This coincides with the inhibition of host gene expression that starts at 6 hpi and becomes almost complete between 9–12 hpi (95). An ectopic and transient expression of nsp1 in mammalian cells is sufficient to promote a robust and global inhibition of host protein synthesis (94,95,147) with a strong reduction of the polysome profile shifting to 80S monosomes (148). The deletion of a small region of the carboxy-terminal part of nsp1 (Δ160–173) is sufficient to reverse the inhibitory effect of the latter and two charged amino acids, K164 and H165, have been identified to be critical for nsp1 function in this translational shutoff (95). Mutation of these two residues into alanine in the SARS-CoV genome to generate the SARS-CoV-mt did not significantly alter viral replication in terms of viral titer, viral RNA transcription or nsp1 expression but it failed to promote robust host endogenous mRNA translation inhibition (95). Partial inhibition of host gene expression was also observed in Vero E6 and 293/ACE2 cells infected by SARS-CoV-mt (95) indicating that either the nsp1-mutant was partially active in the context of infection or that other viral proteins may be involved in this process. Interestingly, SARS-CoV nsp1 targets endogenous cellular mRNAs but also mRNAs resulting from ectopic plasmid expression and transfected mRNAs (94,95). The host cell gene expression shutoff mediated by SARS-CoV nsp1 was not inhibited by actinomycin D treatment that blocked *de novo* RNA synthesis, confirming that nsp1 acts on nascent and pre-existing mRNAs (94,95).

The SARS-CoV nsp1 combines two strategies to inhibit host gene expression: it acts via (i) a direct inhibition of the translation initiation step and (ii) the induction of cellular mRNA degradation (Figure 4). Although translational arrest and cellular degradation are two linked processes, it remains possible to distinguish between them with the use of specific nsp1 mutants (see below). Several evidences indicate that nsp1 interacts with the small 40S ribosomal subunit and this contributes to the reduction of the overall amount of polysomes. This binding is abolished in the case of the specific mutations of the K164 and H165 residues of nsp1 (nsp1-mt) as evidenced by western blot analysis of each fraction in both cellular extracts and rabbit reticulocyte lysate (RRL) (148). In addition, a nsp1 wt-tagged protein, but not the mutant version, co-immunoprecipitates with both S6 ribosomal protein and 18S ribosomal RNA (rRNA) that are key architectural components of the 40S subunit (148). Interestingly, SARS-CoV nsp1 does not appear to be associated with the 80S ribosome suggesting that nsp1 binds exclusively at a pre-initiation stage and is released upon subunit joining. Addition of nsp1 in the RRL affected translation of reporter mRNAs and polysome profile analysis revealed that SARS-CoV nsp1 inhibited 80S ribosome but not 48S initiation complex formation with a critical role for the two charged amino acids in this process (148). As a consequence, translation driven by a cap- and IRES-dependent mechanisms were both inhibited by addition of SARS-CoV nsp1 in RRL. So was the cricket paralysis virus (CrPV) IRES that does not require any of the eIFs and can directly promote the assembly of an 80S ribosome at the AUG codon (149). Therefore, this demonstrates nsp1 targets directly the 40S ribosomal subunit rather than the associated initiation factors.

As mentioned above, SARS-CoV nsp1 also promotes degradation of the host cellular mRNAs in living cells (94,95). Although the mRNAs are also degraded in the RRL, it appears that this does not occur by the same pathway (148). Mutation of two charged and exposed amino acids R124 and K125 of nsp1 (named nsp1-CD for 'cleav-

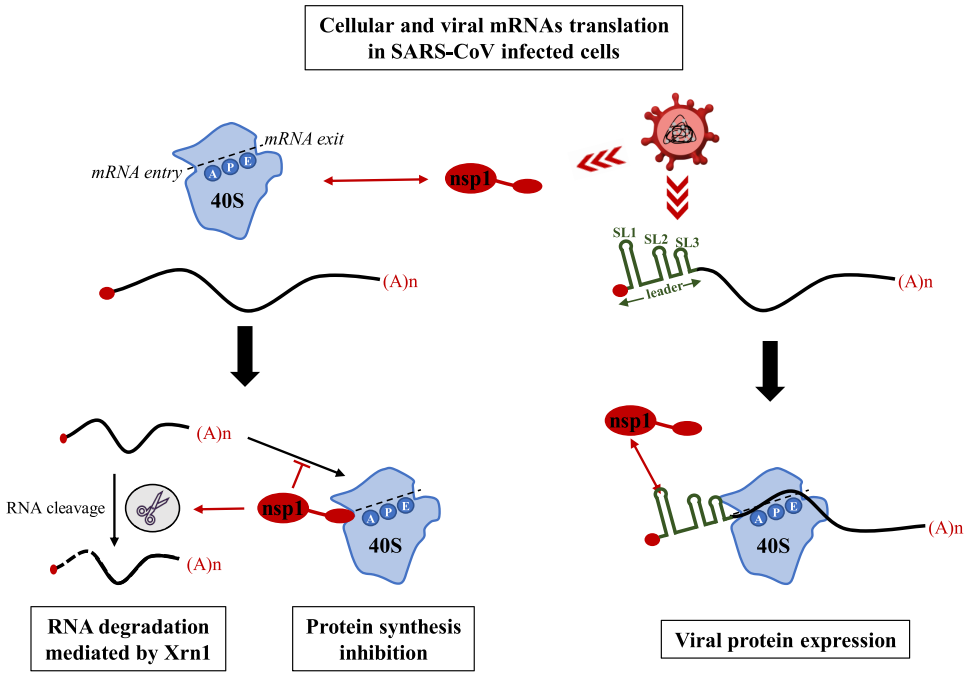

Figure 4. mRNA translation and mRNA decay regulated by SARS-CoV nsp1. A scheme of the 40S ribosomal subunit is showed with the mRNA entry and exit channel and the three tRNA sites: acceptor (A), peptidyl (P) and exit (E). Nsp1 is the first viral protein expressed and is able to interact, through the C-terminal domain, into the mRNA entry channel of the 40S ribosomal subunit. As a result, cellular mRNAs could not be recognized by the ribosome and cellular proteins expression is strongly reduced. In addition, nsp1 promotes endonucleotydic RNA cleavage that conducts the transcript to RNA degradation mediated by Xrn1. In parallel, all SARS-CoV mRNA harbor a common 5′ terminal 72 nt leader sequence with three stem-loop (SL) (labeled in green). SL1 interacts with nsp1 and confers a translational resistance of the viral mRNA to the translation repression mediated by nsp1.

age defective') strongly reduces this cleavage without affecting translation repression both in cell culture and in the RRL suggesting that the two mechanisms are distinct (147). Sucrose gradient density and toeprinting assays are both complementary to measure the ratio of ribosomal complexes associated with the mRNA and to map the position of the ribosome on the mRNA at a nucleotide resolution. Both techniques were used to look at the effect of nsp1-CD on the formation of 48S and 80S initiation complexes on mRNAs translated by either a cap- or an IRES-dependent mechanism: formation of both complexes was inhibited in the RRL in the presence of nsp1-CD (147,148). Interestingly, translation of mRNAs in which initiation was driven by the CrPV or Hepatitis C Virus (HCV) IRESes was repressed by nsp1-wt without any evidence of an RNA cleavage (147,148) suggesting that RNA cleavage could also depend on the structure of the targeted RNA. Indeed, these two IRESes are highly structured (150) and directly bind to the 40S ribosome in the absence of any eIFs (149,151). Addition of nsp1-wt and nsp1-CD to the RRL is sufficient to abolish the binary complex formed between the 40S subunit and the CrPV IRES (147) suggesting a mutually exclusive interaction between the 40S, nsp1 and the IRES structure. In contrast, the interaction of 40S subunit with the HCV IRES was not impaired by the presence of nsp1-wt or nsp1-CD but formation of both 48S and 80S ribosome complexes at the AUG codon was inhibited (147). Cryogenic electron microscopy (cryo-EM) analyses revealed that the HCV IRES interacts with a region of the head and platform edge of the 40S subunit where it partially overlaps with the exit-site (E-site) of the ribosome (152). The CrPV IRES also interacts with the head on the inter-subunit side (153) but, in this case, the CrPV IRES occupies all three tRNA binding sites on the ribosome that are the E-, the peptidyl (P-) and the decoding center (A-) sites (Figure 4, see the 40S ribosome scheme) (154). These difference of occupancy between both IRESes may explain why nsp1 can disrupt the binary complex formed between the 40S subunit and the IRES in the case of CrPV but not with HCV. In agreement with this hypothesis, both Thoms *et al.* and Schubert *et al.* have just shown by cryo-EM studies that nsp1 of a SARS-CoV-2 strain binds to the 40S at the mRNA entry channel (97,98) which is next to the A site (Figure 4). Recent results, obtained by Banerjee *et al.*, show that SARS-CoV-2 nsp1 interacts with the 18S rRNA in a region adjacent to the mRNA entry channel (99). If the structure/function of nsp1 is conserved between the two strains of SARS-CoV, the presence of nsp1 may destabilize the interactions of the CrPV IRES with the ribosome at the A site resulting in the absence of 40S/IRES binary complex.

Endogenous mRNAs, as well as ectopically transfected mRNAs, are both degraded when SARS-CoV nsp1 is expressed in cells (94). However, this is not the case for RNAs that are produced by RNA polymerase type I and III (155). This is consistent with the fact that nsp1 acts through its binding to the 40S subunit and suggests that only mRNAs that are being translated are targeted by nsp1. The Xrn1 protein is a highly conserved 5′–3′ exoribonuclease involved in mRNA degradation in the cytoplasm (156–158). Silencing of Xrn1 in the cell abolishes the effect of transfect-

ing SARS-CoV nsp1 and preserves the integrity of cellular mRNAs (155) indicating that mRNA degradation requires Xrn1 (Figure 4). To our knowledge, Xrn1 is not expressed in the RRL and this could explain why mRNAs are not degraded by nsp1 in this system; however, they are cleaved by others, yet unidentified, endonucleases that are activated by the addition of SARS-CoV nsp1 (Figure 4) (147,148,159). The cleavage sites were then mapped by using a toeprinting approach on reporter mRNAs with the 5′UTR of globin or actin that are both expressed by a cap-dependent mechanism. Addition of SARS-CoV nsp1 to the RRL induced about ten endonucleolytic cleavage prints on both sides of the initiation codon with one or two predominant sites but they failed to highlight a consensus sequence or nucleotide preference (159). However, modification of the RNA secondary and tertiary structures by mutagenesis affected the global pattern of cleavage (159) confirming that the 3-D structure of the RNA plays a role in this process. Then, the authors used a comparison between the EMCV and PV IRESes as both IRESes exhibit differences in their site of initiation relative to the binding site of the 40S ribosomal subunit. Indeed, whereas for EMCV, the 40S binds directly at the vicinity of the AUG codon, this is not the case for the PV IRES in which the initiation codon is located 154 nt downstream to the 3′ border of the IRES (150). Consequently, in PV, the preinitiation complex needs to reach the initiation codon by linear scanning after its primary attachment to the IRES (160). Addition of the SARS-CoV nsp1 induced several endonucleolytic cleavages at the 3′ border of both IRESes but no cleavage could be detected around the authentic AUG codon of the PV mRNA (159) suggesting that the ribosome was stalled after its attachment and could not scan to the initiation codon in the presence of nsp1. This nsp1 mediated RNA cleavage did not occur when both the HCV or CrPV IRESes were used in the RRL (147,159). In the case of CrPV IRES, nsp1 was able to disrupt the binary complex formed between the small ribosomal subunit and the IRES and remained probably bound to the 40S subunit. In such conditions, the mRNA that harbors the CrPV IRES cannot associate with the ribosome and, therefore, was not targeted by nsp1. The situation is even more complex in the case of HCV IRES because a binary complex 40S/IRES was formed in the presence of nsp1 but the RNA remained uncleaved. To date no explanation and experiments have been proposed to understand this resistance to RNA cleavage; however, this IRES is highly structured with pseudoknot structures that could provide a physical barrier against endonucleases. The fact that SARS-CoV nsp1 does not show any intrinsic endonuclease activity means that nsp1 does not act directly on its substrate but rather activates one, or several, unknown cellular endonucleases. As nsp1 blocks ribosomes essentially during the initiation step, these stalled 40S ribosomes on the mRNA may trigger a quality control mechanism that could be reminiscent to the no-go decay which targets mRNAs on which elongation is stalled (161,162). Further studies have to be carried out to understand the molecular mechanism by which nsp1 can induce RNA cleavage.

Nsp1 from others CoV strains. The four different lineages of the β-CoV genera share a relatively low amino acid sequence similarity: for example, SARS-CoV nsp1 shares only 20.6%, 17.9% and 26.1% sequence similarity with MHV, B-CoV and MERS-CoV nsp1 proteins, respectively (89,163). Despite these differences, the amino acid sequence, LRKxGxKG, is relatively well conserved between the nsp1 of SARS-CoV, MHV, B-CoV and MERS-CoV (163,164) and is localized at positions 123–130 in the SARS-CoV nsp1 as a reference. Importantly, this consensus contains the two residues R124 and K125 that are critical for the endonucleolytic cleavage (96).

As for SARS-CoV, MHV nsp1 is localized exclusively in the cytoplasm of infected cells (165) and has been reported to inhibit the expression of reporter genes (166). Northern blot analyses of MHV infected cellular extracts also indicated a massive degradation of host cell mRNAs (85) with deletion of its carboxy-terminal domain being sufficient to abolish nsp1 function (166). Mutation of the consensus sequence in nsp1 results in a decrease of translation of reporter genes (167). The conserved domain (LRKxGxKG) appears to be needed during *in vivo* viral infection as its mutation leads to a strong attenuation of virulence (167) but the precise molecular mechanism by which MHV nsp1 inhibits gene expression awaits determination.

The MERS-CoV nsp1 exerts a dual function on cellular mRNAs by inducing both translation inhibition and mRNA degradation (96,163). The key charged amino acids identified in SARS-CoV nsp1 are conserved in the MERS-CoV and point mutation of the lysine in position 181, which is the analog of lysine 164 in SARS-CoV nsp1 (95), completely abolishes the function of nsp1 (168). Mutation of the two conserved amino acids R146/K147 in MERS-CoV nsp1, which corresponds to residues R124/K125 in SARS-CoV nsp1, recapitulates the cleavage defective effect and allows to dissociate the two functions of the protein (96,147). Despite these functional similarities, MERS-CoV nsp1 shows many differences with SARS-CoV nsp1 notably at the level of cellular localization, the interaction with the 40S ribosomal subunit and the targeted mRNAs (96). Indeed, only mRNAs transcribed by the RNA polymerase type II in the nucleus of the host infected cell are targeted by MERS-CoV nsp1. As such, mRNAs that are injected or engineered to be produced in the cytoplasm are not sensitive to repression or degradation. Interestingly and in contrast to SARS-CoV, MERS-CoV nsp1 is localized both in the nucleus and the cytoplasm and weakly interacts with the 40S ribosomal subunit raising the question of how MERS-CoV nsp1 can act on actively translated mRNAs. Curiously, the expression of mRNAs produced in the cytoplasm was stimulated by the presence of MERS-CoV nsp1 although the mechanism by which this occurred was not solved. A possible explanation could be attributed to a competitive effect due to the cellular shutoff that increases the availability of the components of the translational machinery for these mRNAs.

Nsp1 is also expressed in strains that belong to the α-CoV genus, such as Porcine Epidemic Diarrhea Virus (PEDV), TGEV, HCoV-229E and HCov-NL63 but the protein is significantly smaller (110 aa instead of 180 aa for the SARS-CoV) and sequence alignments show only ∼21% identity and 23% similarity with the first 128 aa of SARS-CoV nsp1 proteins between both HCoV-229E and HCoV-NL63 (93).

However, bioinformatic analysis revealed that the nsp1 proteins of HCoV-229E, HCov-NL63 and SARS-CoV share a very similar 3D shaping structure (93). The crystal structures of TGEV and PEDV nsp1 confirmed a high degree of similarity with SARS-CoV nsp1 despite this lack of sequence homology (92,164,169) indicating a conservation of protein function. In agreement with this, nsp1 of TGEV, PEDV, HCoV-229E and HCov-NL63 strains are able to inhibit global host gene expression at a similar level than the SARS-CoV nsp1 (92,93,159,169). It is also noteworthy that the two K164/H165 residues of SARS-CoV nsp1, which are required for the interaction with the 40S ribosomal subunit (95), are lacking in α-CoV nsp1. However, both HCoV NL63- and HCoV 229E-nsp1 can still immunoprecipitate the S6 ribosomal protein from 293T cell extracts (92,93) suggesting that an interaction between the 40S ribosomal subunit and nsp1 still takes place in α-CoV strains. In addition, TGEV nsp1 cannot induce RNA degradation (159) but HCoV NL63- and 229E-nsp1 are able to do so (93) and several amino acids have been identified in TGEV, PEDV, HCoV-229E and HCov-NL63 strains to be required to promote efficient translation inhibition (92,169). Thus, nsp1-mediated inhibition of protein synthesis during α-CoV infection appears to be a very conserved process despite many differences in the way it is achieved.

SARS-CoV-2 nsp1. Nsp 1 proteins of SARS-CoV and SARS-CoV-2 share 84.4% sequence identity and 93.9% of sequence similarity suggesting a strong conservation at the level of protein function. Infection of human lung epithelial (Calu3) or monkey kidney (Vero) cells with SARS-CoV-2 strain results in a global translation inhibition (99). Transfection of a plasmid coding for the SARS-CoV-2 nsp1 into 293T cells is sufficient to reduce cellular proteins expression level (99) and induces a shift from the polyribosome fractions to 80S monosomes pointing out that a global inhibition of translation occurs in the presence of SARS-CoV-2 nsp1 (97). SARS-CoV-2 nsp1 is associated with both 40S and 80S but not with the polyribosome fractions (97,98). *In vitro* binding assays have confirmed that recombinant SARS-CoV-2 nsp1 can interact with purified 40S but not with the 60S subunit (97,98) and this binding requires both K164 and H165 residues as it was the case for SARS-CoV nsp1 (97,98,148). Furthermore, addition of recombinant nsp1 protein into a cell-free *in vitro* translation system is also sufficient to inhibit expression of reporter mRNAs (97–99). The interaction between nsp1 and the 40S ribosomal subunit has recently been imaged by cryo-EM at an average resolution of 2.6–2.8 Å, and this revealed that the C-terminus of nsp1 was made of two α-helices and located inside the ribosomal mRNA entry channel at the latch structure formed between rRNA helix h18 of the body and h34 of the head and uS3 of the 40S subunit (97,98,170,171). The C-terminal domain of nsp1 interacts specifically with uS3, uS5 and rRNA helix h18 (97–99). The K164 and H165 residues establish a key interaction with helix h18 and the binding of nsp1 to the mRNA entrance channel blocks mRNA entry (Figure 4) (99). Interestingly, the location of nsp1 could inhibit tRNA recruitment to the 80S ribosome that would block the elongation step (99). This could explain the observation that the mRNA was always missing from all purified and analyzed nsp1/ribosomal complexes (97,98). As a consequence, addition of SARS-CoV-2 nsp1 to HeLa translation-competent lysates inhibited translation of reporter mRNAs (97–99) except when they are bearing the SARS-CoV-2 genomic 5′UTR (99).

Other CoV viral proteins

Infection with SARS-CoV strains that encodes nsp1-mt (K164A & H165A) results in the inhibition of host mRNA translation (95) suggesting that other viral proteins are involved in the control of cellular mRNA translation.

A two-hybrid screen in yeast has identified interactions between the f subunit of the initiation factor eIF3 and the SARS-CoV S protein that was later confirmed by immunoprecipitation studies in HeLa cells. The N-terminal region of the S protein (20–404 aa) is sufficient to bind to eIF3f and this modifies the cellular localization of eIF3f that become mainly cytoplasmic likewise the S protein. Addition of a S protein truncated in its C-terminal domain (SΔC) into the reticulocyte lysate is able to inhibit the expression of reporter mRNAs and this can be partially restored by the addition of recombinant eIF3f (90). This translation inhibitory effect of spike protein has also been demonstrated in other CoV strains like IBV (90). However, it can be argued that the work was essentially performed with the SΔC mutant in which the peptide signal is deleted that also affects its localization to the cytoplasm compartment; indeed, within the WT S protein, the N-terminal domain that interacts with eIF3f is localized at the extracellular side of the plasma membrane. Therefore, in such conditions, the S protein is not supposed to be able to interact with initiation factors.

The SARS-CoV nucleocapsid N protein is the most abundant amongst all structural proteins and it harbors an RNA-binding domain in its N-terminal region. A two-hybrid yeast screen has shown that the C-terminal domain can interact with the human elongation factor 1-alpha (EF1α) (172), which is an essential component for the elongation phase of translation (173,174). The N protein can immunoprecipitate native EF1α proteins from cell extracts and this property is conserved with the N protein of the HCoV-229E strain (172). Due to its self-association, the viral N protein can form aggregates that include EF1α (172). Interestingly, HSP70, a chaperone protein that preferentially binds to denatured or aggregated proteins (175), is also found as part of these complexes (172). Thus, it is not surprising that addition of recombinant N protein was able to inhibit translation of reporter mRNAs both in the RRL and in cellular extracts (172). Once again, evidences for inhibition during viral infection are lacking to confirm a function of N protein in the cellular translation shutoff.

Very recently, a global analysis of SARS-CoV-2 host interacting proteins has allowed to identify 332 interactions between viral and human proteins (102). Some of them are involved in translation. For instance, the nsp2 interacts with both GIGYF2 and eIF4E2 (4EHP) (102) that are two components of a complex that represses mRNA translation (176). These interactions were already identified with nsp2 from SARS-CoV (177) but were never investigated further although they suggest a role for nsp2 in regulating mRNA

translation. Similarly, nsp9 interacts also with eIF4H (102), a factor that enhances the ATP dependent helicase activity of eIF4A (178–180). Interestingly, the complex formed between eIF4A and eIF4H can be inactivated using a specific inhibitor that is able to lock eIF4A in an inactive conformation (179). The interaction between nsp9 and eIF4H could modulate eIF4A function and thus, play a role on translational efficiency. Finally, the N protein of SARS-CoV-2 can interact with different isoforms of PABP and the ribosomal protein L36 (102), and this may also participate in the regulation of protein synthesis.

Structure and function of the viral mRNAs

Translation and integrity of cellular mRNAs are significantly altered in cells that are infected by SARS-CoV or MERS-CoV. Despite these conditions, viral mRNAs are not degraded and viral protein synthesis is maintained at high level (95,96,99). In an *in vitro* system, the SARS-CoV nsp1 does not induce the endonucleolytic cleavage on sgRNAs that have been purified from SARS-CoV infected cells (159). These experiments indicate that viral mRNAs could be protected from this host cell shutoff and this may be attributed to RNA *cis*-acting elements that confer this resistance.

In order to better understand this mechanism, it is important to start with a brief description of the architecture of the 5′ and 3′ termini of the CoV genome. The TRSs that are essential for viral genome transcription (43,181) are located downstream to the leader sequence and upstream to the AUG codon (reviewed in (28)). As such, all coronaviral transcripts (depending on the subtype) share an identical coterminal 3′ ends and common 70–90 nt long leader sequences at their 5′ terminus (182). These noncoding RNA regions fold into secondary and tertiary structures that are involved in functional RNA–RNA interactions; they also bind to a subset of viral and cellular proteins during replication and translation. In this part, we will not detail the specific role of these RNA structures that are used for genome replication and we advise readers to consult these excellent reviews on the topic (183,184). Rather, we will focus our attention on RNA structures that are directly involved in translational control of the coronavirus genomic and subgenomic RNAs. Thus, for clarity, we will name '5′UTR' the region spanning from the 5′ terminus of the transcript and up to the AUG codon. The first 60–95 nt of the 5′UTR refer to the leader sequence, which is common to all coronaviral mRNAs.

The viral 5′UTR. Analysis of the RNA structures of the 5′UTR was essentially performed from the MHV strain. Indeed, by using a combination of phylogenetic analysis and computer-based prediction software, the 140 first nucleotides of the MHV genome have initially been modelized to form three conserved stem-loops (SL) that are named SL1, SL2 and SL4 (185,186). A 3 stem-loop folding is also observed for MERS-CoV whereas SARS-CoV and B-CoV contain an additional SL (SL3) that folds the leader TRS (TRS-L) into a hairpin loop. Interestingly, for all of these four members of the β-CoV family, the RNA structure-based models predict that the AUG codon is embedded within SL4 (183). Thus, this suggests that the accessibility of the initiator codon may be an issue as it is not positioned in an unstructured region although this has not yet been formerly experimentally determined. In 2015, Selective 2′-Hydroxyl Acylation analyzed by Primer Extension (SHAPE) analysis of the 5′UTR of MHV revealed a conformational structure that was in good agreement with previous predicted models and confirmed the presence of SL1, SL2 and the correct structure of SL4 at position located between nt 80 and 130 (187). Interestingly, the overall structural conformation of these four β-CoV was very similar despite very poor sequence conservation at the level of primary nucleotide sequence suggesting a link between RNA structure and function (143,186,188). Although the function of the 5′ UTR in replication has been extensively studied, its role in translation remains, yet, to be determined.

The different CoV RNAs are resistant to the endonucleolytic cleavage induced by nsp1 (Figure 4). This was confirmed by *in vitro* studies with purified sgRNA3 and sgRNA9 (159) indicating that they contain *cis*-acting elements that confer resistance. In order to investigate whether the viral UTRs could be involved in the protection against the action of nsp1, Huang and colleagues engineered different versions of the sgRNA9 coding for the SARS-CoV N protein. They monitored translational efficiency of these constructs in the RRL and they found that the viral 5′UTR was sufficient to protect the transcripts against RNA cleavage (159) but not translation inhibition (147). The 5′UTR of the mRNA encoding the N protein harbors the common 72 nt-long sequence leader with an additional stretch of 8 nt. Mutational analysis of the 5′ terminal nucleotides of the leader sequence affected the resistance to the endonucleolytic cleavage indicating that the leader sequence could specifically protect the viral mRNAs. Experiments conducted in cells showed that the leader sequence conferred resistance to both RNA degradation and translation repression induced by nsp1 (189) suggesting that an unidentified cellular partner was required to promote a total resistance to nsp1; this cellular partner would be absent from the RRL. They also showed that nsp1 could specifically interact with SL1 of the leader region and this was sufficient to counteract translational inhibition (Figure 4) (189). Interestingly, the nsp1 amino acid residues needed for 40S binding (K164/H165) and for RNA cleavage (R124/K125) are required to bind SL1 (189). These data confirm that SARS-CoV nsp1 exhibits functional domains involved both in RNA binding and translational regulation, but the molecular mechanism remains unknown. However, as lysine 164 is involved in both viral mRNA and ribosome attachment, we can speculate that these two binding are mutually exclusive and the presence of SL1 on the viral mRNA could displace nsp1 located at the mRNA entry channel (97–99) in order to allow viral protein synthesis (Figure 4). Very recently, Schubert and colleagues have reported that the SARS-CoV-2 nsp1 could also inhibit translation of transcripts harboring the 5′UTR of the gRNA in a HeLa cell free system (98); this was already observed with SARS-CoV nsp1 in a similar experimental setting (159). In contrast, Banerjee and colleagues showed, in a cellular system, that the leader sequence and especially the SL1 structure can protect the mRNA from nsp1-mediated translational inhibition (99).

In addition, the distance between the 5′ cap and the SL1 appears to be critical to counteract the function of nsp1 on the viral mRNAs (99). Therefore, the function of nsp1 on mRNA expression may vary from the experimental translational system used (cells, cellular extracts or RRL).

In contrast, MERS-CoV nsp1 only targets cellular mRNAs that are transcribed into the nucleus of the host with no effect on viral mRNAs synthesized from the cytoplasm. However, if the CoV mRNAs are engineered to be artificially synthesized in the nucleus, these viral mRNAs become targets for nsp1. Interestingly, in this case, they can escape translation repression if they possess the leader sequence harboring the SL1 motif (163). However, this resistance appears to be CoV strain specific as SARS-CoV nsp1 represses MERS-CoV mRNAs despite the presence of the MERS-CoV leader sequence (96); the reciprocal has not been studied. In contrast to SARS-CoV nsp1, MERS-CoV nsp1 requires the N-terminal region and more precisely the arginine at position 13 to interact with the SL1 RNA structure (163). Once again and unlike SARS-CoV-nsp1, MERS-CoV-nsp1 can stimulate expression of viral messengers as well as those produced or injected into the cytoplasm. The cleavage defective mutant nsp1 loses this stimulating activity on viral RNAs indicating that residues R146/K147 are required for the efficient expression of viral RNAs (96).

The different functions of nsp1 from SARS-CoV, SARS-CoV-2 and MERS-CoV strains in the cellular mRNAs translation and decay, and in the viral mRNAs protection are recapitulated in Table 1.

Due to the process of viral replication and transcription (190,191), the 5′UTRs of all viral mRNAs start with a cap moiety followed by a strictly conserved ∼72 nt sequence leader. The size of the entire 5′UTRs ranges from 72 to 264 nt in the case of SARS-CoV mRNAs (192) and from 75 to 275 nt for SARS-CoV-2 mRNAs (Table 2) (14).

As mentioned above, the impact and the role of the 5′ RNA structures on viral protein synthesis remain to be determined. However, it is known that gRNAs and sgRNAs are translated by a canonical cap-dependent translation initiation mechanism and, thus, they require the eIF4F complex: eIF4E, eIF4G and eIF4A. Several studies on different CoVs have studied viral translation in the presence of inhibitors against components of eIF4F. This showed that addition of cap analogue in the RRL strongly reduced translation of reporter mRNAs driven by the 5′UTR derived from the B-CoV strain (193,194), which indicates that eIF4E was required for translation initiation. This result was confirmed by the use of the 4E2RCat compound that inhibited interaction between eIF4E and eIF4G (195) as it almost suppressed HCoV-229E replication with a strong reduction of the expression of the Spike protein (196). Finally, hippuristanol and silvestrol that are two molecules known to specifically inhibit the eIF4A RNA helicase, did also affect HCoV-229E and MERS-CoV replication (196,197). Further analyses showed that this defect of viral replication was due to impairment of viral protein expression (197). Moreover, a comparison of the effects of silvestrol between picornavirus (which are dependent on eIF4A for translation) and HCoV-229E and MERS-CoV showed a stronger sensitivity to silvestrol for coronaviral mRNAs (197).

Interestingly, the initiator AUG codons of most SARS-CoV sgRNAs are surrounded by a poor Kozak context (192) suggesting that a leaky scanning mechanism may occur during viral mRNAs translation initiation. Yang and colleagues have analyzed the ability of these different sgRNA 5′UTR to initiate translation of reporter gene in noninfected cells and they showed that, in such system, leaky scanning was indeed taking place (192). Leaky scanning has been studied in details on the sgRNA7 of both SARS-CoV (198) and B-CoV (193,199) and results in the production of two different proteins from two distinct ORFs. Mutations of the respective AUG codons and/or their nucleotide context impacted their level of expression (193,198,199). In the case of SARS-CoV sgRNA7, the protein ORF7b initiated by leaky scanning was detected in infected cells and incorporated in the viral particle (198). Leaky scanning was also reported from the 5′UTR of the SARS-CoV sgRNA2–1 with recombinant plasmids (192). Analysis of the initiation codons from the different sgRNAs of the SARS-CoV-2 strain shows that several of them are located in a weak Kozak context (namely those initiating for N, S, ORF3a, E and ORF6 proteins) (Table 2). These differences may have an impact on the translation rate and it could also promote expression of unexpected proteins that may be relevant for the virus.

Another layer of complexity in the regulation of translation is provided by the presence of a short uORF located immediately downstream of the genomic leader sequence (Table 2). This uORF is only found on the gRNA, but not on the sgRNAs (200) although this bears some exceptions (201), suggesting that translation of genomic and subgenomic RNAs can be regulated by distinct mechanisms. This uORF potentially encodes a short peptide (3–13 aa) and is found in the vast majority of CoV genomes as established on a sampling of 38 reference strains (200). Based on *in vitro* translation studies, the authors showed that the MHV uORF downregulated translational efficiency from the major ORF1 start codon (200). Ribosomal profiling studies confirmed that this uORF was read by incoming ribosomes during MHV infection despite its weak initiation context (202). Interestingly, MHV mutant viruses lacking this structure showed similar growth properties than the WT but, after 10 passages, all mutants in which the uORF was altered, reverted to the WT sequence or generated a new uORF sequence. This suggests that this uORF plays a beneficial, although nonessential, role in replication. In addition, this effect was exerted at the level of translation as reversion to another uORF resulted in the synthesis of a different short peptide that the one encoded from the WT virus. Mutation of the AUG codon of the uORF in MHV and B-CoV 5′UTR resulted in the enhancement of translation of the main ORF (201,203,204) indicating that it could be a way to control the flux of ribosomes on the mRNA to regulate the level of expression of the nonstructural proteins.

In the case of SARS-CoV, all viral mRNAs start with the same 72 nt leader sequence suggesting a common mechanism for initial ribosome binding. However, the gRNA and the sgRNAs exhibit differences in the length and structure of the untranslated region downstream to nucleotide 72 and up to nucleotide 264 (205). These differences may affect ribosomal scanning and, consequently, translational

Table 1. Comparison of the nsp 1 functional characteristics between SARS-CoV, SARS-CoV-2 and MERS-CoV strains; ND, not determined

	Nsp1 functions	SARS-CoV	SARS-CoV-2	MERS-CoV
General characteristics	Sequence identity with SARS-CoV-2	84.4%	100%	∼25%
	Cellular localization	Cytoplasmic		Nuclear and cytoplasmic
Translation shutoff	Shutoff	Yes		Yes
	40S binding	Yes: The C-terminal domain of nsp1 binds at the mRNA entry channel of the 40S ribosome		No
	Critical amino acids	K164/H165		K181
Cellular mRNA degradation	mRNAs targeted	All mRNAs	ND	Only mRNAs transcribed in the nucleus
	Critical amino acids	R124/K125	ND	R164/K165
Viral mRNA escape	*Cis*-acting element required	SL1 (leader sequence)	SL1 (leader sequence)	SL1 (leader sequence)
	Critical amino acids	R124	ND	R13

Table 2. Translational characteristics of the SARS-CoV-2 transcripts

Transcript		ORF	5′UTR length (nt)	AUG initiation codon context	uORF
gRNA		ORF1a and ORF1ab: nsps	265	**a**ag *AUG***G**	ugc *AUG* C
sgRNA	S-RNA	Spike (S)	76	**a**ca *AUG* U	no
	3a-RNA	ORF3a	77	cuu *AUG***G**	no
	E-RNA	Envelope (E)	77	cuu *AUG* U	no
	M-RNA	Membrane (M)	119	**g**cc *AUG***G**	no
	6-RNA	ORF6	230	cag *AUG* U	no
	7a-RNA	ORF7a	75	**a**ac *AUG* A	no
	7b-RNA	ORF7b	151	**a**ga *AUG* A	no
	8-RNA	ORF8	75	**a**ac *AUG* A	no
	N-RNA	Nucleocapsid (N)	83	**a**aa *AUG* U	no

efficiency. Although most transcripts have only a few nucleotides extension downstream to the leader sequence, this is not the case for the gRNA and sgRNAs 5, 6 and 8 that have a longer extension of 264, 116, 227 and 155 nt, respectively (192,205). Yang and colleagues have constructed reporter RNAs bearing these 5′UTRs and they compared their translational efficiency. Some 5′UTRs promote a weaker expression of the reporter gene confirming that this region, together with the nucleotide context surrounding the AUG, can impact the translation rate of viral mRNAs (192). Such a difference in expression has also been pointed out in B-CoV in which the length of the 5′UTR of the gRNA and sgRNA 7 are 210 and 77 nt long, respectively. The presence of these additional 133 nt in the 5′UTR of the gRNA is sufficient to significantly decrease the expression of a reporter gene (194). Transcriptomic studies in SARS-CoV-2 infected cells have shown that 10 sgRNA are produced in addition to the gRNA (14). The leader sequence is 72 nt long and the size of the 5′UTR of most sgRNA is similar to the sequence leader (between 75 and 83 nt) but, for three of them (the gRNA, sgRNA5 and sgRNA6), they are 265, 119 and 230 nt long, respectively (Table 2).

The viral 3′UTR. The 3′UTR of coronaviruses has a size that ranges between 300 and 500 nt in length from the stop codon to the beginning of the poly(A) tail. Most of this 3′UTR (436 nt in MHV, 492 nt for TGEV, 338 nt for IBV) is essential for viral replication as it plays a critical role in negative strand RNA synthesis (31,206–208). There has been a lot of studies using biochemical and computer-based algorithms combined with functional studies to modelize the structure and explore the function of the various motifs that are present in the 3′ UTR. This has led to a model initially described for MHV (209) that postulates that the 68 nt just downstream to the stop codon of the N gene folds into a bulged stem loop (BSL), which is followed by a 54 nt hairpin-type pseudoknot (210). These two structures, BSL and pseudoknot, are phylogenetically conserved in length and shape (but, likewise for the RNA structures in the 5′UTR, not at the level of nucleotide sequence) among all coronaviruses studied so far and were proposed to function as a molecular switch during viral RNA synthesis (211). Other secondary and tertiary structures are also found downstream to the pseudoknot but these motifs are less well conserved among strains and appear, for most part, not to be essential for viral replication (for a review see (183)).

The poly(A) tail at the 3′ terminus of the transcript also plays a critical role in mRNA stability and translation through its interaction with PABP (212–214). Cytoplasmic PABP interacts both with the deadenylation machinery and most of the translation initiation factors. Thus, the length of the poly(A) tail can modulate expression of mRNAs, and cytoplasmic polyadenylation can occur to regulate translation (215,216). As it is also a target for deadenylases leading to RNA decay and loss of viral genome integrity, the length of the poly(A) tail of viral RNA has to be thoroughly controlled. Nevertheless, the mechanisms implicated in coronaviral RNA polyadenylation remain unclear. It is assumed that the poly(A) tail is probably generated from a short poly(U) stretch template found in the negative-strand genome by using a slippage mechanism involving the viral RNA-dependent RNA polymerase; alternatively, the virus could also use the cytoplasmic poly(A)-polymerase in an AAUAAA-independent manner. Indeed, the canonical

polyadenylation signal (AAUAAA) is not present in CoV mRNAs but it is not required if the mRNA already possesses a short poly(A) stretch. Here, the poly(U) stretch can be used as a template for a short poly(A) synthesis by the viral replicase or the cellular transcriptase (217). It is noteworthy that Peng *et al*. have described the presence of an AGUAAA noncanonical polyadenylation signal that is not required for efficient coronavirus mRNA polyadenylation but may be critical when the length of the tail becomes too short (218).

A dynamic regulation of the control of poly(A) tail length has also been reported in the course of viral infection when the length of the poly(A) tail in the B-CoV strain extends from a 45 (A) at the beginning of infection to a 65 (A) stretch later on during the cycle (219). Interestingly, this length variation was similarly found with IBV infection that suggests a common mechanism among coronaviruses that can occur both in cell culture and in the host organism (220). It is well known that changes in poly(A) tail length are often associated with changes in translational regulation. In the case of coronavirus mRNAs translation, transcripts with longer poly(A) tail are more efficiently translated (219). Moreover, it has been shown that nsp8 from HCoV-229E exhibits an adenyltransferase activity that indicates for a possible role for the protein in the extension of the viral poly(A) tail (221).

Interactions between viral and host factors with the poly(A) tail have been studied and reports show that cellular PABP can bind to the coronaviral poly(A) tail (222). More recently, data support evidence that the B-CoV N protein can also bind to the poly(A) tail with a high affinity to compete with PABP. As a result, the N protein inhibits mRNA translation in a poly(A)-dependent manner in both the RRL and cultured cells (223). Interestingly, the N protein can interact with both PABP and eIF4G and pulldown assays suggest that the presence of N protein may alter the interaction between eIF4G and eIF4E (223). To summarize, multiple interactions between the ploy(A) tail, PABP and N protein occur during CoV infection and contribute to regulate translation of cellular mRNAs. In addition, the N protein interacts with nsp9 (223), which is a replicase protein associated with the viral polymerase (224); Thus, the poly(A) tail may act as a regulator to coordinate the use of the viral genome for translation (binding to PABP) or for replication (binding to N).

Finally, a recent study using transcriptomic analysis has confirmed that SARS-CoV-2 RNAs are polyadenylated with a median length of 47 (A) residues (14). This poly(A) tail is longer for gRNAs than for sgRNAs and among the sgRNAs, two populations are observed: a minor one that harbors a ∼30 A residues and a major one that contains a poly(A) tail of about 45 residues. Transcripts with the short poly(A) tail may represent a population of RNAs that have already engaged in the first processes of deadenylation and RNA decay. Interestingly, an epitranscriptomic analysis of the RNA modifications, mainly N6-methyladenosine (m6A) but also 5-methylcytosine methylation (5mC), 2′-0-methylation (Nm), deamination and terminal uridylation shows that all these modified RNAs exhibit shorter poly(A) tail compared to unmodified RNAs. This observation confirms that viral RNA modifications are involved in viral RNA stability and translational control through the length of the poly(A) tail (14).

To conclude this chapter, the interactions between the two termini were shown to play some role both in viral replication and translation. Indeed, the model of discontinuous transcription of subgenomic RNAs implies that 5′ and 3′ interactions are needed for efficient replication (225–227). In TGEV, these interactions occur via RNA–RNA, RNA–protein and protein–protein contacts and induce circularization of the coronavirus genome to promote elongation of the minus strand (228). However, more related to the topic of this review, other RNA–protein interactions have been evidenced (222) and suggested that the PABP bound to the 3′ poly(A) tail also contributes to genome circularization with its ability to interact with eIF4G (222). Thus, it suggests that molecular interactions mediated by the 5′ and 3′ UTRs are important for CoV translation and it would be essential, in the future, to define better the nature and function of these interactions between RNAs and potential viral and cellular proteins involved in the process.

CONCLUDING REMARKS

Like in many RNA viruses, protein synthesis is controlled at different levels during CoVs infection. As we have seen, one of the most comprehensive mechanisms is probably translation repression mediated by nsp1. Recent cryo-EM studies have revealed novel insights in how SARS-CoV-2 nsp1 interferes with ribosome function (97,98). However, RNA cleavage and/or degradation induced by nsp1 remains a mystery. In addition, the mechanism by which translational repression is mediated in MERS-CoV nsp1 and α-CoV nsp1 remains to be determined. For clarity and as a summary, we have recapitulated in Table 1 the different functions fulfilled by nsp1 from SARS-CoV, SARS-CoV-2 and MERS-CoV strains.

Based on the NMR structure of SARS-CoV nsp1 (164), Jauregui and colleagues have engineered 38 mutants that target 62 exposed amino acids and analyzed their ability to promote inhibition of host gene expression. From this work, they identified versions of the nsp1 protein that abolished, attenuated or increased the inhibition of host gene expression (229). These data confirm that coronaviruses are able to evolve through mutation of these residues.

Interestingly, SARS-CoV nsp1 can also disrupt localization of the nuclear pore complex protein Nup93 (230), which is consistent with its perinuclear localization (94,231). As a consequence, nsp1 alters the nuclear-cytoplasmic distribution of nucleolin (230). As nucleolin is an RNA binding protein implicated in RNA stability (232), its delocalization in the presence of nsp1 could contribute to the control of host gene expression mediated by nsp1. Interaction between SARS-CoV-2 nsp1 and Nup93 has not been detected from the analysis of SARS-CoV-2 human protein–protein interactome but the authors showed that both nsp9 and ORF6 protein are able to interact with nuclear pore components (102).

Recent data providing from ribosome profiling assays, performed in SARS-CoV-2 infected cells, added an additional layer of complexity in the regulation of translation from the gRNA and sgRNAs. Indeed, the authors have

identified 23 novel ORFs including internal in-frame and out-frame ORFs, and several uORFs that make the translation of these mRNAs more complex and require further functional investigations (27).

To conclude, it is also important to mention recent data on epitranscriptomic of CoV RNAs. To date, 172 RNA modifications can be listed (233) in which the m6A that remains predominant and which is known to play critical roles in mRNA metabolism such as mRNA stability, decay and translation (234). As a result, m6A RNA modification of both viral and cellular mRNAs is a new mean to control post-transcriptional gene expression during viral infection (235). However, the effects of m6A modifications can either promote viral replication as it is the case for enterovirus 71, influenza A virus and the human immunodeficiency virus, but it can also negatively impact viral production as demonstrated during both HCV and ZIKV infection (235). M6A modifications have been studied in cells infected with the α-CoV PEDV strain and the authors showed a decrease in demethylation activity that correlates with an increase of m6A addition in the host cellular RNAs resulting in a decrease of PEDV replication (236). The RNA genome of SARS-CoV-2 contains >50 potential m6A sites based on the presence of specific sequence motifs for m6A modification by the RNA methylase complex METTL3/14 (237). Gain or loss of m6A results in significant functional changes during viral replication (235) and it will be important to determine precisely whether it has a pro- or antiviral effect.

So, the recent data provided by ribosome profiling assay in SARS-CoV-2 infected cells (27), the SARS-CoV-2 protein interactome (102) and the potential mRNA epitranscriptomic regulation confirm the importance of the relationship that exists between the viral proteins and the components of the translational machinery.

FUNDING

Agence nationale de recherche sur le sida et les hépatites virale (ANRS). Funding for open access charge: Institut national de la santé et de la recherche médicale (INSERM).
Conflict of interest statement. None declared.

REFERENCES

1. Lefkowitz,E.J., Dempsey,D.M., Hendrickson,R.C., Orton,R.J., Siddell,S.G. and Smith,D.B. (2018) Virus taxonomy: the database of the International Committee on Taxonomy of Viruses (ICTV). *Nucleic Acids Res.*, **46**, D708–D717.
2. Hamre,D. and Procknow,J.J. (1966) A new virus isolated from the human respiratory tract. *Proc. Soc. Exp. Biol. Med.*, **121**, 190–193.
3. McIntosh,K., Becker,W.B. and Chanock,R.M. (1967) Growth in suckling-mouse brain of "IBV-like" viruses from patients with upper respiratory tract disease. *PNAS*, **58**, 2268–2273.
4. Tyrrell,D.A. and Bynoe,M.L. (1965) Cultivation of a novel type of Common-Cold virus in organ cultures. *Br. Med. J.*, **1**, 1467–1470.
5. van der Hoek,L., Pyrc,K., Jebbink,M.F., Vermeulen-Oost,W., Berkhout,R.J., Wolthers,K.C., Wertheim-van Dillen,P.M., Kaandorp,J., Spaargaren,J. and Berkhout,B. (2004) Identification of a new human coronavirus. *Nat. Med.*, **10**, 368–373.
6. Woo,P.C., Lau,S.K., Chu,C.M., Chan,K.H., Tsoi,H.W., Huang,Y., Wong,B.H., Poon,R.W., Cai,J.J., Luk,W.K. *et al.* (2005) Characterization and complete genome sequence of a novel coronavirus, coronavirus HKU1, from patients with pneumonia. *J. Virol.*, **79**, 884–895.
7. Rota,P.A., Oberste,M.S., Monroe,S.S., Nix,W.A., Campagnoli,R., Icenogle,J.P., Penaranda,S., Bankamp,B., Maher,K., Chen,M.H. *et al.* (2003) Characterization of a novel coronavirus associated with severe acute respiratory syndrome. *Science*, **300**, 1394–1399.
8. Marra,M.A., Jones,S.J., Astell,C.R., Holt,R.A., Brooks-Wilson,A., Butterfield,Y.S., Khattra,J., Asano,J.K., Barber,S.A., Chan,S.Y. *et al.* (2003) The Genome sequence of the SARS-associated coronavirus. *Science*, **300**, 1399–1404.
9. Ksiazek,T.G., Erdman,D., Goldsmith,C.S., Zaki,S.R., Peret,T., Emery,S., Tong,S., Urbani,C., Comer,J.A., Lim,W. *et al.* (2003) A novel coronavirus associated with severe acute respiratory syndrome. *N. Engl. J. Med.*, **348**, 1953–1966.
10. Bermingham,A., Chand,M.A., Brown,C.S., Aarons,E., Tong,C., Langrish,C., Hoschler,K., Brown,K., Galiano,M., Myers,R. *et al.* (2012) Severe respiratory illness caused by a novel coronavirus, in a patient transferred to the United Kingdom from the Middle East, September 2012. *Euro Surveill.*, **17**, 20290.
11. Lu,G. and Liu,D. (2012) SARS-like virus in the Middle East: a truly bat-related coronavirus causing human diseases. *Protein Cell*, **3**, 803–805.
12. Zaki,A.M., van Boheemen,S., Bestebroer,T.M., Osterhaus,A.D. and Fouchier,R.A. (2012) Isolation of a novel coronavirus from a man with pneumonia in Saudi Arabia. *N. Engl. J. Med.*, **367**, 1814–1820.
13. Dong,E., Du,H. and Gardner,L. (2020) An interactive web-based dashboard to track COVID-19 in real time. *Lancet Infect. Dis.*, **20**, 533–534.
14. Kim,D., Lee,J.Y., Yang,J.S., Kim,J.W., Kim,V.N. and Chang,H. (2020) The architecture of SARS-CoV-2 transcriptome. *Cell*, **181**, 914–921.
15. Zhou,P., Yang,X.L., Wang,X.G., Hu,B., Zhang,L., Zhang,W., Si,H.R., Zhu,Y., Li,B., Huang,C.L. *et al.* (2020) A pneumonia outbreak associated with a new coronavirus of probable bat origin. *Nature*, **579**, 270–273.
16. Kim,J.M., Chung,Y.S., Jo,H.J., Lee,N.J., Kim,M.S., Woo,S.H., Park,S., Kim,J.W., Kim,H.M. and Han,M.G. (2020) Identification of coronavirus isolated from a patient in Korea with COVID-19. *Osong. Public Health Res. Perspect.*, **11**, 3–7.
17. Cheever,F.S. and Daniels,J.B. *et al.* (1949) A murine virus (JHM) causing disseminated encephalomyelitis with extensive destruction of myelin. *J. Exp. Med.*, **90**, 181–210.
18. Mebus,C.A., Stair,E.L., Rhodes,M.B. and Twiehaus,M.J. (1973) Neonatal calf diarrhea: propagation, attenuation, and characteristics of a coronavirus-like agent. *Am. J. Vet. Res.*, **34**, 145–150.
19. Mebus,C.A., Stair,E.L., Rhodes,M.B. and Twiehaus,M.J. (1973) Pathology of neonatal calf diarrhea induced by a coronavirus-like agent. *Vet. Pathol.*, **10**, 45–64.
20. Jacks,T. and Varmus,H.E. (1985) Expression of the Rous sarcoma virus pol gene by ribosomal frameshifting. *Science*, **230**, 1237–1242.
21. Brierley,I., Boursnell,M.E., Binns,M.M., Bilimoria,B., Blok,V.C., Brown,T.D. and Inglis,S.C. (1987) An efficient ribosomal frame-shifting signal in the polymerase-encoding region of the coronavirus IBV. *EMBO J.*, **6**, 3779–3785.
22. Giedroc,D.P. and Cornish,P.V. (2009) Frameshifting RNA pseudoknots: structure and mechanism. *Virus Res.*, **139**, 193–208.
23. Plant,E.P. and Dinman,J.D. (2008) The role of programmed-1 ribosomal frameshifting in coronavirus propagation. *Front. Biosci. J. Virtual Lib.*, **13**, 4873–4881.
24. Atkins,J.F. and Baranov,P.V. (2013) Molecular biology: Antibiotic re-frames decoding. *Nature*, **503**, 478–479.
25. Dinman,J.D. (2012) Mechanisms and implications of programmed translational frameshifting. *Wiley Interdiscipl. Rev. RNA*, **3**, 661–673.
26. Kelly,J.A., Olson,A.N., Neupane,K., Munshi,S., San Emeterio,J., Pollack,L., Woodside,M.T. and Dinman,J.D. (2020) Structural and functional conservation of the programmed -1 ribosomal frameshift signal of SARS coronavirus 2 (SARS-CoV-2). *J. Biol. Chem.*, **295**, 10741–10748.
27. Finkel,Y., Mizrahi,O., Nachshon,A., Weingarten-Gabbay,S., Morgenstern,D., Yahalom-Ronen,Y., Tamir,H., Achdout,H., Stein,D., Israeli,O. *et al.* (2020) The coding capacity of SARS-CoV-2. *Nature*, doi:10.1038/s41586-020-2739-1.
28. Sola,I., Almazan,F., Zuniga,S. and Enjuanes,L. (2015) Continuous and discontinuous RNA synthesis in coronaviruses. *Ann. Rev. Virol.*, **2**, 265–288.

29. Liao,C.L. and Lai,M.M. (1992) RNA recombination in a coronavirus: recombination between viral genomic RNA and transfected RNA fragments. *J. Virol.*, **66**, 6117–6124.
30. Viehweger,A., Krautwurst,S., Lamkiewicz,K., Madhugiri,R., Ziebuhr,J., Holzer,M. and Marz,M. (2019) Direct RNA nanopore sequencing of full-length coronavirus genomes provides novel insights into structural variants and enables modification analysis. *Genome Res.*, **29**, 1545–1554.
31. Luytjes,W., Gerritsma,H. and Spaan,W.J. (1996) Replication of synthetic defective interfering RNAs derived from coronavirus mouse hepatitis virus-A59. *Virology*, **216**, 174–183.
32. den Boon,J.A. and Ahlquist,P. (2010) Organelle-like membrane compartmentalization of positive-strand RNA virus replication factories. *Annu. Rev. Microbiol.*, **64**, 241–256.
33. Wolff,G., Limpens,R., Zevenhoven-Dobbe,J.C., Laugks,U., Zheng,S., de Jong,A.W.M., Koning,R.I., Agard,D.A., Grunewald,K., Koster,A.J. *et al.* (2020) A molecular pore spans the double membrane of the coronavirus replication organelle. *Science*, **369**, 1395–1398.
34. Wolff,G., Melia,C.E., Snijder,E.J. and Barcena,M. (2020) Double-Membrane vesicles as platforms for viral replication. *Trends Microbiol.*, **28**, 1022–1033.
35. Knoops,K., Kikkert,M., Worm,S.H., Zevenhoven-Dobbe,J.C., van der Meer,Y., Koster,A.J., Mommaas,A.M. and Snijder,E.J. (2008) SARS-coronavirus replication is supported by a reticulovesicular network of modified endoplasmic reticulum. *PLoS Biol.*, **6**, e226.
36. Ulasli,M., Verheije,M.H., de Haan,C.A. and Reggiori,F. (2010) Qualitative and quantitative ultrastructural analysis of the membrane rearrangements induced by coronavirus. *Cell. Microbiol.*, **12**, 844–861.
37. de Wilde,A.H., Raj,V.S., Oudshoorn,D., Bestebroer,T.M., van Nieuwkoop,S., Limpens,R., Posthuma,C.C., van der Meer,Y., Barcena,M., Haagmans,B.L. *et al.* (2013) MERS-coronavirus replication induces severe in vitro cytopathology and is strongly inhibited by cyclosporin A or interferon-alpha treatment. *J. Gen. Virol.*, **94**, 1749–1760.
38. Doyle,N., Hawes,P.C., Simpson,J., Adams,L.H. and Maier,H.J. (2019) The porcine deltacoronavirus replication organelle comprises Double-Membrane vesicles and zippered endoplasmic reticulum with Double-Membrane spherules. *Viruses*, **11**, 1030.
39. Oudshoorn,D., Rijs,K., Limpens,R., Groen,K., Koster,A.J., Snijder,E.J., Kikkert,M. and Barcena,M. (2017) Expression and cleavage of middle east respiratory syndrome coronavirus nsp3-4 Polyprotein induce the formation of Double-Membrane vesicles that mimic those associated with coronaviral RNA replication. *mBio*, **8**, e01658-17.
40. Krijnse-Locker,J., Ericsson,M., Rottier,P.J. and Griffiths,G. (1994) Characterization of the budding compartment of mouse hepatitis virus: evidence that transport from the RER to the Golgi complex requires only one vesicular transport step. *J. Cell Biol.*, **124**, 55–70.
41. Jain,J., Gaur,S., Chaudhary,Y. and Kaul,R. (2020) The molecular biology of intracellular events during Coronavirus infection cycle. *VirusDisease*, **31**, 1–5.
42. Fehr,A.R. and Perlman,S. (2015) Coronaviruses: an overview of their replication and pathogenesis. *Methods Mol. Biol.*, **1282**, 1–23.
43. Masters,P.S. (2006) The molecular biology of coronaviruses. *Adv. Virus Res.*, **66**, 193–292.
44. Weiss,S.R. and Navas-Martin,S. (2005) Coronavirus pathogenesis and the emerging pathogen severe acute respiratory syndrome coronavirus. *Microbiol. Mol. Biol. Rev.*, **69**, 635–664.
45. Hartenian,E., Nandakumar,D., Lari,A., Ly,M., Tucker,J.M. and Glaunsinger,B.A. (2020) The molecular virology of coronaviruses. *J. Biol. Chem.*, **295**, 12910–12934.
46. Asano,K. (2014) Why is start codon selection so precise in eukaryotes? *Translation*, **2**, e28387.
47. Llacer,J.L., Hussain,T., Marler,L., Aitken,C.E., Thakur,A., Lorsch,J.R., Hinnebusch,A.G. and Ramakrishnan,V. (2015) Conformational differences between open and closed states of the Eukaryotic translation initiation complex. *Mol. Cell*, **59**, 399–412.
48. Obayashi,E., Luna,R.E., Nagata,T., Martin-Marcos,P., Hiraishi,H., Singh,C.R., Erzberger,J.P., Zhang,F., Arthanari,H., Morris,J. *et al.* (2017) Molecular landscape of the ribosome Pre-initiation complex during mRNA Scanning: Structural role for eIF3c and its control by eIF5. *Cell Rep.*, **18**, 2651–2663.
49. Herrmannova,A., Prilepskaja,T., Wagner,S., Sikrova,D., Zeman,J., Poncova,K. and Valasek,L.S. (2020) Adapted formaldehyde gradient cross-linking protocol implicates human eIF3d and eIF3c, k and l subunits in the 43S and 48S pre-initiation complex assembly, respectively. *Nucleic Acids Res.*, **48**, 1969–1984.
50. Gallie,D.R. (1991) The cap and poly(A) tail function synergistically to regulate mRNA translational efficiency. *Genes Dev.*, **5**, 2108–2116.
51. Wells,S.E., Hillner,P.E., Vale,R.D. and Sachs,A.B. (1998) Circularization of mRNA by eukaryotic translation initiation factors. *Mol. Cell*, **2**, 135–140.
52. Archer,S.K., Shirokikh,N.E., Hallwirth,C.V., Beilharz,T.H. and Preiss,T. (2015) Probing the closed-loop model of mRNA translation in living cells. *RNA Biol.*, **12**, 248–254.
53. Algire,M.A., Maag,D. and Lorsch,J.R. (2005) Pi release from eIF2, not GTP hydrolysis, is the step controlled by start-site selection during eukaryotic translation initiation. *Mol. Cell*, **20**, 251–262.
54. Majumdar,R. and Maitra,U. (2005) Regulation of GTP hydrolysis prior to ribosomal AUG selection during eukaryotic translation initiation. *EMBO J.*, **24**, 3737–3746.
55. Shirokikh,N.E. and Preiss,T. (2018) Translation initiation by cap-dependent ribosome recruitment: Recent insights and open questions. *Wiley Interdiscipl. Rev. RNA*, **9**, e1473.
56. Merrick,W.C. and Pavitt,G.D. (2018) Protein synthesis initiation in Eukaryotic cells. *Cold Spring Harb. Perspect. Biol.*, **10**, a033092.
57. Pelletier,J. and Sonenberg,N. (2019) The organizing principles of Eukaryotic ribosome recruitment. *Annu. Rev. Biochem.*, **88**, 307–335.
58. Advani,V.M. and Ivanov,P. (2019) Translational control under Stress: Reshaping the translatome. *Bioessays*, **41**, e1900009.
59. Anderson,P. and Kedersha,N. (2008) Stress granules: the Tao of RNA triage. *Trends Biochem. Sci.*, **33**, 141–150.
60. Kedersha,N., Ivanov,P. and Anderson,P. (2013) Stress granules and cell signaling: more than just a passing phase? *Trends Biochem. Sci.*, **38**, 494–506.
61. McCormick,C. and Khaperskyy,D.A. (2017) Translation inhibition and stress granules in the antiviral immune response. *Nat. Rev. Immunol.*, **17**, 647–660.
62. Kozak,M. (1989) Context effects and inefficient initiation at non-AUG codons in eucaryotic cell-free translation systems. *Mol. Cell. Biol.*, **9**, 5073–5080.
63. Kozak,M. (1987) At least six nucleotides preceding the AUG initiator codon enhance translation in mammalian cells. *J. Mol. Biol.*, **196**, 947–950.
64. Kozak,M. (1986) Point mutations define a sequence flanking the AUG initiator codon that modulates translation by eukaryotic ribosomes. *Cell*, **44**, 283–292.
65. Pisarev,A.V., Kolupaeva,V.G., Pisareva,V.P., Merrick,W.C., Hellen,C.U. and Pestova,T.V. (2006) Specific functional interactions of nucleotides at key -3 and +4 positions flanking the initiation codon with components of the mammalian 48S translation initiation complex. *Genes Dev.*, **20**, 624–636.
66. Couso,J.P. and Patraquim,P. (2017) Classification and function of small open reading frames. *Nat. Rev. Mol. Cell Biol.*, **18**, 575–589.
67. Wek,R.C. (2018) Role of eIF2alpha kinases in translational control and adaptation to cellular stress. *Cold Spring Harb. Perspect. Biol.*, **10**, a032870.
68. Chikashige,Y., Kato,H., Thornton,M., Pepper,W., Hilgers,M., Cecil,A., Asano,I., Yamada,H., Mori,C., Brunkow,C. *et al.* (2020) Gcn2 eIF2alpha kinase mediates combinatorial translational regulation through nucleotide motifs and uORFs in target mRNAs. *Nucleic Acids Res.*, **48**, 8977–8992.
69. Johnstone,T.G., Bazzini,A.A. and Giraldez,A.J. (2016) Upstream ORFs are prevalent translational repressors in vertebrates. *EMBO J.*, **35**, 706–723.
70. Schneider,W.M., Chevillotte,M.D. and Rice,C.M. (2014) Interferon-stimulated genes: a complex web of host defenses. *Annu. Rev. Immunol.*, **32**, 513–545.
71. Acosta,P.L., Byrne,A.B., Hijano,D.R. and Talarico,L.B. (2020) Human Type I Interferon Antiviral Effects in Respiratory and Reemerging Viral Infections. *J. Immunol. Res.*, **2020**, 1372494.
72. Chiang,H.S. and Liu,H.M. (2018) The molecular basis of viral inhibition of IRF- and STAT-Dependent immune responses. *Front. Immunol.*, **9**, 3086.
73. Walsh,D. and Mohr,I. (2011) Viral subversion of the host protein synthesis machinery. *Nat. Rev. Microbiol.*, **9**, 860–875.

74. Gradi,A., Svitkin,Y.V., Imataka,H. and Sonenberg,N. (1998) Proteolysis of human eukaryotic translation initiation factor eIF4GII, but not eIF4GI, coincides with the shutoff of host protein synthesis after poliovirus infection. *PNAS*, **95**, 11089–11094.
75. de Breyne,S., Bonderoff,J.M., Chumakov,K.M., Lloyd,R.E. and Hellen,C.U. (2008) Cleavage of eukaryotic initiation factor eIF5B by enterovirus 3C proteases. *Virology*, **378**, 118–122.
76. Rivera,C.I. and Lloyd,R.E. (2008) Modulation of enteroviral proteinase cleavage of poly(A)-binding protein (PABP) by conformation and PABP-associated factors. *Virology*, **375**, 59–72.
77. Roberts,L.O., Jopling,C.L., Jackson,R.J. and Willis,A.E. (2009) Viral strategies to subvert the mammalian translation machinery. *Prog. Mol. Biol. Transl. Sci.*, **90**, 313–367.
78. Kwan,T. and Thompson,S.R. (2019) Noncanonical translation initiation in Eukaryotes. *Cold Spring Harb. Perspect. Biol.*, **11**, a032672.
79. Walker,A.P. and Fodor,E. (2019) Interplay between influenza virus and the host RNA polymerase II transcriptional machinery. *Trends Microbiol.*, **27**, 398–407.
80. Plotch,S.J., Bouloy,M., Ulmanen,I. and Krug,R.M. (1981) A unique cap(m7GpppXm)-dependent influenza virion endonuclease cleaves capped RNAs to generate the primers that initiate viral RNA transcription. *Cell*, **23**, 847–858.
81. Ventoso,I., Sanz,M.A., Molina,S., Berlanga,J.J., Carrasco,L. and Esteban,M. (2006) Translational resistance of late alphavirus mRNA to eIF2alpha phosphorylation: a strategy to overcome the antiviral effect of protein kinase PKR. *Genes Dev.*, **20**, 87–100.
82. Toribio,R., Diaz-Lopez,I., Boskovic,J. and Ventoso,I. (2016) An RNA trapping mechanism in Alphavirus mRNA promotes ribosome stalling and translation initiation. *Nucleic Acids Res.*, **44**, 4368–4380.
83. Siddell,S.G., Wege,H., Barthel,A. and ter Meulen,V. (1980) Coronavirus JHM: cell-free synthesis of structural protein p60. *J. Virol.*, **33**, 10–17.
84. Rottier,P.J., Horzinek,M.C. and van der Zeijst,B.A. (1981) Viral protein synthesis in mouse hepatitis virus strain A59-infected cells: effect of tunicamycin. *J. Virol.*, **40**, 350–357.
85. Hilton,A., Mizzen,L., MacIntyre,G., Cheley,S. and Anderson,R. (1986) Translational control in murine hepatitis virus infection. *J. Gen. Virol.*, **67**, 923–932.
86. Tahara,S.M., Dietlin,T.A., Bergmann,C.C., Nelson,G.W., Kyuwa,S., Anthony,R.P. and Stohlman,S.A. (1994) Coronavirus translational regulation: leader affects mRNA efficiency. *Virology*, **202**, 621–630.
87. Raaben,M., Groot Koerkamp,M.J., Rottier,P.J. and de Haan,C.A. (2007) Mouse hepatitis coronavirus replication induces host translational shutoff and mRNA decay, with concomitant formation of stress granules and processing bodies. *Cell. Microbiol.*, **9**, 2218–2229.
88. Huang,C., Lokugamage,K.G., Rozovics,J.M., Narayanan,K., Semler,B.L. and Makino,S. (2011) Alphacoronavirus transmissible gastroenteritis virus nsp1 protein suppresses protein translation in mammalian cells and in cell-free HeLa cell extracts but not in rabbit reticulocyte lysate. *J. Virol.*, **85**, 638–643.
89. Tohya,Y., Narayanan,K., Kamitani,W., Huang,C., Lokugamage,K. and Makino,S. (2009) Suppression of host gene expression by nsp1 proteins of group 2 bat coronaviruses. *J. Virol.*, **83**, 5282–5288.
90. Xiao,H., Xu,L.H., Yamada,Y. and Liu,D.X. (2008) Coronavirus spike protein inhibits host cell translation by interaction with eIF3f. *PLoS One*, **3**, e1494.
91. Kint,J., Langereis,M.A., Maier,H.J., Britton,P., van Kuppeveld,F.J., Koumans,J., Wiegertjes,G.F. and Forlenza,M. (2016) Infectious bronchitis coronavirus limits interferon production by inducing a host shutoff that requires accessory protein 5b. *J. Virol.*, **90**, 7519–7528.
92. Shen,Z., Ye,G., Deng,F., Wang,G., Cui,M., Fang,L., Xiao,S., Fu,Z.F. and Peng,G. (2018) Structural basis for the inhibition of host gene expression by porcine epidemic diarrhea virus nsp1. *J. Virol.*, **92**, e01896-17.
93. Wang,Y., Shi,H., Rigolet,P., Wu,N., Zhu,L., Xi,X.G., Vabret,A., Wang,X. and Wang,T. (2010) Nsp1 proteins of group I and SARS coronaviruses share structural and functional similarities. *Infect. Genet. Evol.*, **10**, 919–924.
94. Kamitani,W., Narayanan,K., Huang,C., Lokugamage,K., Ikegami,T., Ito,N., Kubo,H. and Makino,S. (2006) Severe acute respiratory syndrome coronavirus nsp1 protein suppresses host gene expression by promoting host mRNA degradation. *PNAS*, **103**, 12885–12890.
95. Narayanan,K., Huang,C., Lokugamage,K., Kamitani,W., Ikegami,T., Tseng,C.T. and Makino,S. (2008) Severe acute respiratory syndrome coronavirus nsp1 suppresses host gene expression, including that of type I interferon, in infected cells. *J. Virol.*, **82**, 4471–4479.
96. Lokugamage,K.G., Narayanan,K., Nakagawa,K., Terasaki,K., Ramirez,S.I., Tseng,C.T. and Makino,S. (2015) Middle east respiratory syndrome coronavirus nsp1 inhibits host gene expression by selectively targeting mRNAs transcribed in the nucleus while sparing mRNAs of cytoplasmic origin. *J. Virol.*, **89**, 10970–10981.
97. Thoms,M., Buschauer,R., Ameismeier,M., Koepke,L., Denk,T., Hirschenberger,M., Kratzat,H., Hayn,M., Mackens-Kiani,T., Cheng,J. *et al.* (2020) Structural basis for translational shutdown and immune evasion by the Nsp1 protein of SARS-CoV-2. *Science*, **369**, 1249–1255.
98. Schubert,K., Karousis,E.D., Jomaa,A., Scaiola,A., Echeverria,B., Gurzeler,L.A., Leibundgut,M., Thiel,V., Muhlemann,O. and Ban,N. (2020) SARS-CoV-2 Nsp1 binds the ribosomal mRNA channel to inhibit translation. *Nat. Struct. Mol. Biol.*, **27**, 959–966.
99. Banerjee,A.K., Blanco,M.R., Bruce,E.A., Honson,D.D., Chen,L.M., Chow,A., Bhat,P., Ollikainen,N., Quinodoz,S.A., Loney,C. *et al.* (2020) SARS-CoV-2 disrupts splicing, translation, and protein trafficking to suppress host defenses. *Cell*, **183**, 1325–1339.
100. Chan,C.P., Siu,K.L., Chin,K.T., Yuen,K.Y., Zheng,B. and Jin,D.Y. (2006) Modulation of the unfolded protein response by the severe acute respiratory syndrome coronavirus spike protein. *J. Virol.*, **80**, 9279–9287.
101. Hetz,C., Zhang,K. and Kaufman,R.J. (2020) Mechanisms, regulation and functions of the unfolded protein response. *Nat. Rev. Mol. Cell Biol.*, **21**, 421–438.
102. Gordon,D.E., Jang,G.M., Bouhaddou,M., Xu,J., Obernier,K., White,K.M., O'Meara,M.J., Rezelj,V.V., Guo,J.Z., Swaney,D.L. *et al.* (2020) A SARS-CoV-2 protein interaction map reveals targets for drug repurposing. *Nature*, **583**, 459–468.
103. Fung,T.S. and Liu,D.X. (2019) Human Coronavirus: Host-Pathogen interaction. *Annu. Rev. Microbiol.*, **73**, 529–557.
104. Perrier,A., Bonnin,A., Desmarets,L., Danneels,A., Goffard,A., Rouille,Y., Dubuisson,J. and Belouzard,S. (2019) The C-terminal domain of the MERS coronavirus M protein contains a trans-Golgi network localization signal. *J. Biol. Chem.*, **294**, 14406–14421.
105. Shajahan,A., Supekar,N.T., Gleinich,A.S. and Azadi,P. (2020) Deducing the N- and O- glycosylation profile of the spike protein of novel coronavirus SARS-CoV-2. *Glycobiology*, doi:10.1093/glycob/cwaa042.
106. Oostra,M., de Haan,C.A., de Groot,R.J. and Rottier,P.J. (2006) Glycosylation of the severe acute respiratory syndrome coronavirus triple-spanning membrane proteins 3a and M. *J. Virol.*, **80**, 2326–2336.
107. Versteeg,G.A., van de Nes,P.S., Bredenbeek,P.J. and Spaan,W.J. (2007) The coronavirus spike protein induces endoplasmic reticulum stress and upregulation of intracellular chemokine mRNA concentrations. *J. Virol.*, **81**, 10981–10990.
108. Reggiori,F., Monastyrska,I., Verheije,M.H., Cali,T., Ulasli,M., Bianchi,S., Bernasconi,R., de Haan,C.A. and Molinari,M. (2010) Coronaviruses Hijack the LC3-I-positive EDEMosomes, ER-derived vesicles exporting short-lived ERAD regulators, for replication. *Cell Host Microbe*, **7**, 500–508.
109. Stertz,S., Reichelt,M., Spiegel,M., Kuri,T., Martinez-Sobrido,L., Garcia-Sastre,A., Weber,F. and Kochs,G. (2007) The intracellular sites of early replication and budding of SARS-coronavirus. *Virology*, **361**, 304–315.
110. Galluzzi,L., Diotallevi,A. and Magnani,M. (2017) Endoplasmic reticulum stress and unfolded protein response in infection by intracellular parasites. *Future Sci. OA*, **3**, FSO198.
111. Smith,J.A. (2014) A new paradigm: innate immune sensing of viruses via the unfolded protein response. *Front. Microbiol.*, **5**, 222.
112. He,B. (2006) Viruses, endoplasmic reticulum stress, and interferon responses. *Cell Death Differ.*, **13**, 393–403.

113. Krahling,V., Stein,D.A., Spiegel,M., Weber,F. and Muhlberger,E. (2009) Severe acute respiratory syndrome coronavirus triggers apoptosis via protein kinase R but is resistant to its antiviral activity. *J. Virol.*, **83**, 2298–2309.
114. Minakshi,R., Padhan,K., Rani,M., Khan,N., Ahmad,F. and Jameel,S. (2009) The SARS Coronavirus 3a protein causes endoplasmic reticulum stress and induces ligand-independent downregulation of the type 1 interferon receptor. *PLoS One*, **4**, e8342.
115. Siu,K.L., Chan,C.P., Kok,K.H., Woo,P.C. and Jin,D.Y. (2014) Comparative analysis of the activation of unfolded protein response by spike proteins of severe acute respiratory syndrome coronavirus and human coronavirus HKU1. *Cell Biosci.*, **4**, 3.
116. Nakagawa,K., Narayanan,K., Wada,M. and Makino,S. (2018) Inhibition of stress granule formation by middle east respiratory syndrome coronavirus 4a accessory protein facilitates viral translation, leading to efficient virus replication. *J. Virol.*, **92**, e00902-18.
117. Deng,X., Hackbart,M., Mettelman,R.C., O'Brien,A., Mielech,A.M., Yi,G., Kao,C.C. and Baker,S.C. (2017) Coronavirus nonstructural protein 15 mediates evasion of dsRNA sensors and limits apoptosis in macrophages. *PNAS*, **114**, E4251–E4260.
118. Kindler,E., Gil-Cruz,C., Spanier,J., Li,Y., Wilhelm,J., Rabouw,H.H., Zust,R., Hwang,M., V'Kovski,P., Stalder,H. *et al.* (2017) Early endonuclease-mediated evasion of RNA sensing ensures efficient coronavirus replication. *PLoS Pathog.*, **13**, e1006195.
119. Rabouw,H.H., Langereis,M.A., Knaap,R.C., Dalebout,T.J., Canton,J., Sola,I., Enjuanes,L., Bredenbeek,P.J., Kikkert,M., de Groot,R.J. *et al.* (2016) Middle East respiratory coronavirus accessory protein 4a inhibits PKR-Mediated antiviral stress responses. *PLoS Pathog.*, **12**, e1005982.
120. Favreau,D.J., Meessen-Pinard,M., Desforges,M. and Talbot,P.J. (2012) Human coronavirus-induced neuronal programmed cell death is cyclophilin d dependent and potentially caspase dispensable. *J. Virol.*, **86**, 81–93.
121. Ivanov,P., Kedersha,N. and Anderson,P. (2019) Stress granules and processing bodies in translational control. *Cold Spring Harb. Perspect. Biol.*, **11**, a032813.
122. Riggs,C.L., Kedersha,N., Ivanov,P. and Anderson,P. (2020) Mammalian stress granules and P bodies at a glance. *J. Cell Sci.*, **133**, jcs242487.
123. Corbet,G.A. and Parker,R. (2019) RNP Granule Formation: Lessons from P-Bodies and stress granules. *Cold Spring Harb. Symp. Quant. Biol.*, **84**, 203–215.
124. Protter,D.S.W. and Parker,R. (2016) Principles and properties of stress granules. *Trends Cell Biol.*, **26**, 668–679.
125. Eiermann,N., Haneke,K., Sun,Z., Stoecklin,G. and Ruggieri,A. (2020) Dance with the Devil: Stress granules and signaling in antiviral responses. *Viruses*, **12**, 984.
126. Tsai,W.C. and Lloyd,R.E. (2014) Cytoplasmic RNA granules and viral infection. *Ann. Rev. Virol.*, **1**, 147–170.
127. Sola,I., Mateos-Gomez,P.A., Almazan,F., Zuniga,S. and Enjuanes,L. (2011) RNA-RNA and RNA-protein interactions in coronavirus replication and transcription. *RNA Biol.*, **8**, 237–248.
128. Peng,T.Y., Lee,K.R. and Tarn,W.Y. (2008) Phosphorylation of the arginine/serine dipeptide-rich motif of the severe acute respiratory syndrome coronavirus nucleocapsid protein modulates its multimerization, translation inhibitory activity and cellular localization. *FEBS J.*, **275**, 4152–4163.
129. Mizutani,T., Fukushi,S., Murakami,M., Hirano,T., Saijo,M., Kurane,I. and Morikawa,S. (2004) Tyrosine dephosphorylation of STAT3 in SARS coronavirus-infected Vero E6 cells. *FEBS Lett.*, **577**, 187–192.
130. Mizutani,T., Fukushi,S., Saijo,M., Kurane,I. and Morikawa,S. (2004) Phosphorylation of p38 MAPK and its downstream targets in SARS coronavirus-infected cells. *Biochem. Biophys. Res. Commun.*, **319**, 1228–1234.
131. Banerjee,S., Narayanan,K., Mizutani,T. and Makino,S. (2002) Murine coronavirus replication-induced p38 mitogen-activated protein kinase activation promotes interleukin-6 production and virus replication in cultured cells. *J. Virol.*, **76**, 5937–5948.
132. McKendrick,L., Thompson,E., Ferreira,J., Morley,S.J. and Lewis,J.D. (2001) Interaction of eukaryotic translation initiation factor 4G with the nuclear cap-binding complex provides a link between nuclear and cytoplasmic functions of the m(7) guanosine cap. *Mol. Cell. Biol.*, **21**, 3632–3641.
133. Knauf,U., Tschopp,C. and Gram,H. (2001) Negative regulation of protein translation by mitogen-activated protein kinase-interacting kinases 1 and 2. *Mol. Cell. Biol.*, **21**, 5500–5511.
134. Pyronnet,S., Imataka,H., Gingras,A.C., Fukunaga,R., Hunter,T. and Sonenberg,N. (1999) Human eukaryotic translation initiation factor 4G (eIF4G) recruits mnk1 to phosphorylate eIF4E. *EMBO J.*, **18**, 270–279.
135. Lachance,P.E.D., Miron,M., Raught,B., Sonenberg,N. and Lasko,P. (2002) Phosphorylation of eukaryotic translation initiation factor 4E is critical for growth. *Mol. Cell. Biol.*, **22**, 1656–1663.
136. Panja,D., Kenney,J.W., D'Andrea,L., Zalfa,F., Vedeler,A., Wibrand,K., Fukunaga,R., Bagni,C., Proud,C.G. and Bramham,C.R. (2014) Two-Stage translational control of dentate gyrus LTP consolidation is mediated by sustained BDNF-TrkB signaling to MNK. *Cell Rep.*, **9**, 1430–1445.
137. Bramham,C.R., Jensen,K.B. and Proud,C.G. (2016) Tuning specific translation in cancer metastasis and synaptic Memory: Control at the MNK-eIF4E Axis. *Trends Biochem. Sci.*, **41**, 847–858.
138. Kopecky-Bromberg,S.A., Martinez-Sobrido,L. and Palese,P. (2006) 7a protein of severe acute respiratory syndrome coronavirus inhibits cellular protein synthesis and activates p38 mitogen-activated protein kinase. *J. Virol.*, **80**, 785–793.
139. Padhan,K., Minakshi,R., Bin Towheed,M.A. and Jameel,S. (2008) Severe acute respiratory syndrome coronavirus 3a protein activates the mitochondrial death pathway through p38 MAP kinase activation. *J. Gen. Virol.*, **89**, 1960–1969.
140. Kono,M., Tatsumi,K., Imai,A.M., Saito,K., Kuriyama,T. and Shirasawa,H. (2008) Inhibition of human coronavirus 229E infection in human epithelial lung cells (L132) by chloroquine: Involvement of p38 MAPK and ERK. *Antiviral Res.*, **77**, 150–152.
141. Proud,C.G. (2019) Phosphorylation and signal transduction pathways in translational control. *Cold Spring Harb. Perspect. Biol.*, **11**, a033050.
142. Lim,Y.X., Ng,Y.L., Tam,J.P. and Liu,D.X. (2016) Human Coronaviruses: A review of Virus-Host interactions. *Diseases*, **4**, 26.
143. Chen,S.C. and Olsthoorn,R.C. (2010) Group-specific structural features of the 5′-proximal sequences of coronavirus genomic RNAs. *Virology*, **401**, 29–41.
144. Bouhaddou,M., Memon,D., Meyer,B., White,K.M., Rezelj,V.V., Marrero,M.C., Polacco,B.J., Melnyk,J.E., Ulferts,S., Kaake,R.M. *et al.* (2020) The global phosphorylation landscape of SARS-CoV-2 infection. *Cell*, **182**, 685–712.
145. Narayanan,K., Ramirez,S.I., Lokugamage,K.G. and Makino,S. (2015) Coronavirus nonstructural protein 1: Common and distinct functions in the regulation of host and viral gene expression. *Virus Res.*, **202**, 89–100.
146. Prentice,E., Jerome,W.G., Yoshimori,T., Mizushima,N. and Denison,M.R. (2004) Coronavirus replication complex formation utilizes components of cellular autophagy. *J. Biol. Chem.*, **279**, 10136–10141.
147. Lokugamage,K.G., Narayanan,K., Huang,C. and Makino,S. (2012) Severe acute respiratory syndrome coronavirus protein nsp1 is a novel eukaryotic translation inhibitor that represses multiple steps of translation initiation. *J. Virol.*, **86**, 13598–13608.
148. Kamitani,W., Huang,C., Narayanan,K., Lokugamage,K.G. and Makino,S. (2009) A two-pronged strategy to suppress host protein synthesis by SARS coronavirus Nsp1 protein. *Nat. Struct. Mol. Biol.*, **16**, 1134–1140.
149. Wilson,J.E., Pestova,T.V., Hellen,C.U. and Sarnow,P. (2000) Initiation of protein synthesis from the A site of the ribosome. *Cell*, **102**, 511–520.
150. Balvay,L., Soto Rifo,R., Ricci,E.P., Decimo,D. and Ohlmann,T. (2009) Structural and functional diversity of viral IRESes. *Biochim. Biophys. Acta*, **1789**, 542–557.
151. Pestova,T.V., Shatsky,I.N., Fletcher,S.P., Jackson,R.J. and Hellen,C.U. (1998) A prokaryotic-like mode of cytoplasmic eukaryotic ribosome binding to the initiation codon during internal translation initiation of hepatitis C and classical swine fever virus RNAs. *Genes Dev.*, **12**, 67–83.

152. Quade,N., Boehringer,D., Leibundgut,M., van den Heuvel,J. and Ban,N. (2015) Cryo-EM structure of Hepatitis C virus IRES bound to the human ribosome at 3.9-A resolution. *Nat. Commun.*, **6**, 7646.
153. Spahn,C.M., Jan,E., Mulder,A., Grassucci,R.A., Sarnow,P. and Frank,J. (2004) Cryo-EM visualization of a viral internal ribosome entry site bound to human ribosomes: the IRES functions as an RNA-based translation factor. *Cell*, **118**, 465–475.
154. Johnson,A.G., Grosely,R., Petrov,A.N. and Puglisi,J.D. (2017) Dynamics of IRES-mediated translation. *Philos. Trans. R. Soc. Lon. Series B, Biol. Sci.*, **372**, 20160177.
155. Gaglia,M.M., Covarrubias,S., Wong,W. and Glaunsinger,B.A. (2012) A common strategy for Host RNA degradation by divergent viruses. *J. Virol.*, **86**, 9527–9530.
156. Nagarajan,V.K., Jones,C.I., Newbury,S.F. and Green,P.J. (2013) XRN 5′ → 3′ exoribonucleases: Structure, mechanisms and functions. *Bba-Gene Regul. Mech.*, **1829**, 590–603.
157. Perez-Ortin,J.E., Alepuz,P., Chavez,S. and Choder,M. (2013) Eukaryotic mRNA Decay: Methodologies, pathways, and links to other stages of gene expression. *J. Mol. Biol.*, **425**, 3750–3775.
158. Labno,A., Tomecki,R. and Dziembowski,A. (2016) Cytoplasmic RNA decay pathways - Enzymes and mechanisms. *Bba-Mol. Cell Res*, **1863**, 3125–3147.
159. Huang,C., Lokugamage,K.G., Rozovics,J.M., Narayanan,K., Semler,B.L. and Makino,S. (2011) SARS coronavirus nsp1 protein induces template-dependent endonucleolytic cleavage of mRNAs: viral mRNAs are resistant to nsp1-induced RNA cleavage. *PLoS Pathog.*, **7**, e1002433.
160. Sweeney,T.R., Abaeva,I.S., Pestova,T.V. and Hellen,C.U. (2014) The mechanism of translation initiation on Type 1 picornavirus IRESs. *EMBO J.*, **33**, 76–92.
161. Powers,K.T., Szeto,J.A. and Schaffitzel,C. (2020) New insights into no-go, non-stop and nonsense-mediated mRNA decay complexes. *Curr. Opin. Struct. Biol.*, **65**, 110–118.
162. Navickas,A., Chamois,S., Saint-Fort,R., Henri,J., Torchet,C. and Benard,L. (2020) No-Go Decay mRNA cleavage in the ribosome exit tunnel produces 5′-OH ends phosphorylated by Trl1. *Nat. Commun.*, **11**, 122.
163. Terada,Y., Kawachi,K., Matsuura,Y. and Kamitani,W. (2017) MERS coronavirus nsp1 participates in an efficient propagation through a specific interaction with viral RNA. *Virology*, **511**, 95–105.
164. Almeida,M.S., Johnson,M.A., Herrmann,T., Geralt,M. and Wuthrich,K. (2007) Novel beta-barrel fold in the nuclear magnetic resonance structure of the replicase nonstructural protein 1 from the severe acute respiratory syndrome coronavirus. *J. Virol.*, **81**, 3151–3161.
165. Brockway,S.M., Lu,X.T., Peters,T.R., Dermody,T.S. and Denison,M.R. (2004) Intracellular localization and protein interactions of the gene 1 protein p28 during mouse hepatitis virus replication. *J. Virol.*, **78**, 11551–11562.
166. Zust,R., Cervantes,L., Weber,F., Kuri,T., Davidson,A., Siddell,S.G., Ludewig,B. and Thiel,V. (2007) Interaction of mouse hepatitis non-strutural protein 1 with innate immune effector pathways. *Swiss Med. Wkly.*, **137**, 35s.
167. Lei,L., Ying,S., Baojun,L., Yi,Y. and Xiang,H. (2014) Attenuation of mouse hepatitis virus by deletion of the LLRKxGxKG region of Nsp1 (vol 8, e61166, 2013). *PLoS One*, **9**, e61166.
168. Nakagawa,K., Narayanan,K., Wada,M., Popov,V.L., Cajimat,M., Baric,R.S. and Makino,S. (2018) The Endonucleolytic RNA cleavage function of nsp1 of middle east respiratory syndrome coronavirus promotes the production of infectious virus particles in specific human cell lines. *J. Virol.*, **92**, e01157-18.
169. Shen,Z., Wang,G., Yang,Y.L., Shi,J.L., Fang,L.R., Li,F., Xiao,S.B., Fu,Z.F. and Peng,G.Q. (2019) A conserved region of nonstructural protein 1 from alphacoronaviruses inhibits host gene expression and is critical for viral virulence. *J. Biol. Chem.*, **294**, 13606–13618.
170. Ben-Shem,A., Garreau de Loubresse,N., Melnikov,S., Jenner,L., Yusupova,G. and Yusupov,M. (2011) The structure of the eukaryotic ribosome at 3.0 A resolution. *Science*, **334**, 1524–1529.
171. Weisser,M. and Ban,N. (2019) Extensions, extra factors, and extreme Complexity: Ribosomal structures provide insights into Eukaryotic translation. *Cold Spring Harb. Perspect. Biol.*, **11**, a032367.
172. Zhou,B., Liu,J., Wang,Q., Liu,X., Li,X., Li,P., Ma,Q. and Cao,C. (2008) The nucleocapsid protein of severe acute respiratory syndrome coronavirus inhibits cell cytokinesis and proliferation by interacting with translation elongation factor 1alpha. *J. Virol.*, **82**, 6962–6971.
173. Riis,B., Rattan,S.I., Clark,B.F. and Merrick,W.C. (1990) Eukaryotic protein elongation factors. *Trends Biochem. Sci.*, **15**, 420–424.
174. Hotokezaka,Y., Tobben,U., Hotokezaka,H., Van Leyen,K., Beatrix,B., Smith,D.H., Nakamura,T. and Wiedmann,M. (2002) Interaction of the eukaryotic elongation factor 1A with newly synthesized polypeptides. *J. Biol. Chem.*, **277**, 18545–18551.
175. Rosenzweig,R., Nillegoda,N.B., Mayer,M.P. and Bukau,B. (2019) The Hsp70 chaperone network. *Nat. Rev. Mol. Cell Biol.*, **20**, 665–680.
176. Morita,M., Ler,L.W., Fabian,M.R., Siddiqui,N., Mullin,M., Henderson,V.C., Alain,T., Fonseca,B.D., Karashchuk,G., Bennett,C.F. *et al.* (2012) A novel 4EHP-GIGYF2 translational repressor complex is essential for mammalian development. *Mol. Cell. Biol.*, **32**, 3585–3593.
177. Cornillez-Ty,C.T., Liao,L.J., Yates,J.R., Kuhn,P. and Buchmeier,M.J. (2009) Severe acute respiratory syndrome coronavirus nonstructural protein 2 interacts with a host protein complex involved in mitochondrial biogenesis and intracellular signaling. *J. Virol.*, **83**, 10314–10318.
178. Marintchev,A. (2013) Roles of helicases in translation initiation: a mechanistic view. *Biochim. Biophys. Acta*, **1829**, 799–809.
179. Sun,Y., Atas,E., Lindqvist,L.M., Sonenberg,N., Pelletier,J. and Meller,A. (2014) Single-molecule kinetics of the eukaryotic initiation factor 4AI upon RNA unwinding. *Structure*, **22**, 941–948.
180. Rogers,G.W. Jr., Richter,N.J., Lima,W.F. and Merrick,W.C. (2001) Modulation of the helicase activity of eIF4A by eIF4B, eIF4H, and eIF4F. *J. Biol. Chem.*, **276**, 30914–30922.
181. Brian,D.A. and Baric,R.S. (2005) Coronavirus genome structure and replication. *Curr. Top. Microbiol. Immunol.*, **287**, 1–30.
182. Spaan,W., Delius,H., Skinner,M., Armstrong,J., Rottier,P., Smeekens,S., van der Zeijst,B.A. and Siddell,S.G. (1983) Coronavirus mRNA synthesis involves fusion of non-contiguous sequences. *EMBO J.*, **2**, 1839–1844.
183. Yang,D. and Leibowitz,J.L. (2015) The structure and functions of coronavirus genomic 3′ and 5′ ends. *Virus Res.*, **206**, 120–133.
184. Madhugiri,R., Fricke,M., Marz,M. and Ziebuhr,J. (2016) Coronavirus cis-Acting RNA Elements. *Adv. Virus Res.*, **96**, 127–163.
185. Kang,H., Feng,M., Schroeder,M.E., Giedroc,D.P. and Leibowitz,J.L. (2006) Stem-loop 1 in the 5′ UTR of the SARS coronavirus can substitute for its counterpart in mouse hepatitis virus. *Adv. Exp. Med. Biol.*, **581**, 105–108.
186. Liu,P., Li,L., Millership,J.J., Kang,H., Leibowitz,J.L. and Giedroc,D.P. (2007) A U-turn motif-containing stem-loop in the coronavirus 5′ untranslated region plays a functional role in replication. *RNA*, **13**, 763–780.
187. Yang,D., Liu,P., Wudeck,E.V., Giedroc,D.P. and Leibowitz,J.L. (2015) SHAPE analysis of the RNA secondary structure of the Mouse Hepatitis Virus 5′ untranslated region and N-terminal nsp1 coding sequences. *Virology*, **475**, 15–27.
188. Kang,H., Feng,M., Schroeder,M.E., Giedroc,D.P. and Leibowitz,J.L. (2006) Putative cis-acting stem-loops in the 5′ untranslated region of the severe acute respiratory syndrome coronavirus can substitute for their mouse hepatitis virus counterparts. *J. Virol.*, **80**, 10600–10614.
189. Tanaka,T., Kamitani,W., DeDiego,M.L., Enjuanes,L. and Matsuura,Y. (2012) Severe acute respiratory syndrome coronavirus nsp1 facilitates efficient propagation in cells through a specific translational shutoff of host mRNA. *J. Virol.*, **86**, 11128–11137.
190. Lai,M.M., Brayton,P.R., Armen,R.C., Patton,C.D., Pugh,C. and Stohlman,S.A. (1981) Mouse hepatitis virus A59: mRNA structure and genetic localization of the sequence divergence from hepatotropic strain MHV-3. *J. Virol.*, **39**, 823–834.
191. Lai,M.M., Patton,C.D. and Stohlman,S.A. (1982) Replication of mouse hepatitis virus: negative-stranded RNA and replicative form RNA are of genome length. *J. Virol.*, **44**, 487–492.
192. Yang,Y., Hussain,S., Wang,H., Ke,M. and Guo,D. (2009) Translational control of the subgenomic RNAs of severe acute respiratory syndrome coronavirus. *Virus Genes*, **39**, 10–18.
193. Senanayake,S.D. and Brian,D.A. (1997) Bovine coronavirus I protein synthesis follows ribosomal scanning on the bicistronic N mRNA. *Virus Res.*, **48**, 101–105.

194. Senanayake,S.D. and Brian,D.A. (1999) Translation from the 5′ untranslated region (UTR) of mRNA 1 is repressed, but that from the 5′ UTR of mRNA 7 is stimulated in coronavirus-infected cells. *J. Virol.*, **73**, 8003–8009.
195. Cencic,R., Hall,D.R., Robert,F., Du,Y., Min,J., Li,L., Qui,M., Lewis,I., Kurtkaya,S., Dingledine,R. *et al.* (2011) Reversing chemoresistance by small molecule inhibition of the translation initiation complex eIF4F. *PNAS*, **108**, 1046–1051.
196. Cencic,R., Desforges,M., Hall,D.R., Kozakov,D., Du,Y., Min,J., Dingledine,R., Fu,H., Vajda,S., Talbot,P.J. *et al.* (2011) Blocking eIF4E-eIF4G interaction as a strategy to impair coronavirus replication. *J. Virol.*, **85**, 6381–6389.
197. Muller,C., Ulyanova,V., Ilinskaya,O., Pleschka,S. and Shah Mahmud,R. (2017) A Novel Antiviral Strategy against MERS-CoV and HCoV-229E Using Binase to Target Viral Genome Replication. *Bionanoscience*, **7**, 294–299.
198. Schaecher,S.R., Mackenzie,J.M. and Pekosz,A. (2007) The ORF7b protein of severe acute respiratory syndrome coronavirus (SARS-CoV) is expressed in virus-infected cells and incorporated into SARS-CoV particles. *J. Virol.*, **81**, 718–731.
199. Senanayake,S.D., Hofmann,M.A., Maki,J.L. and Brian,D.A. (1992) The nucleocapsid protein gene of bovine coronavirus is bicistronic. *J. Virol.*, **66**, 5277–5283.
200. Wu,H.Y., Guan,B.J., Su,Y.P., Fan,Y.H. and Brian,D.A. (2014) Reselection of a genomic upstream open reading frame in mouse hepatitis coronavirus 5′-untranslated-region mutants. *J. Virol.*, **88**, 846–858.
201. Hofmann,M.A., Senanayake,S.D. and Brian,D.A. (1993) An intraleader open reading frame is selected from a hypervariable 5′ terminus during persistent infection by the bovine coronavirus. *Adv. Exp. Med. Biol.*, **342**, 105–109.
202. Irigoyen,N., Firth,A.E., Jones,J.D., Chung,B.Y., Siddell,S.G. and Brierley,I. (2016) High-Resolution analysis of coronavirus gene expression by RNA sequencing and ribosome profiling. *PLoS Pathog.*, **12**, e1005473.
203. Chen,W. and Baric,R.S. (1995) Function of a 5′-end genomic RNA mutation that evolves during persistent mouse hepatitis virus infection in vitro. *J. Virol.*, **69**, 7529–7540.
204. Hofmann,M.A., Senanayake,S.D. and Brian,D.A. (1993) A translation-attenuating intraleader open reading frame is selected on coronavirus mRNAs during persistent infection. *PNAS*, **90**, 11733–11737.
205. Hussain,S., Pan,J., Chen,Y., Yang,Y., Xu,J., Peng,Y., Wu,Y., Li,Z., Zhu,Y., Tien,P. *et al.* (2005) Identification of novel subgenomic RNAs and noncanonical transcription initiation signals of severe acute respiratory syndrome coronavirus. *J. Virol.*, **79**, 5288–5295.
206. Lin,Y.J. and Lai,M.M. (1993) Deletion mapping of a mouse hepatitis virus defective interfering RNA reveals the requirement of an internal and discontiguous sequence for replication. *J. Virol.*, **67**, 6110–6118.
207. Dalton,K., Casais,R., Shaw,K., Stirrups,K., Evans,S., Britton,P., Brown,T.D. and Cavanagh,D. (2001) cis-acting sequences required for coronavirus infectious bronchitis virus defective-RNA replication and packaging. *J. Virol.*, **75**, 125–133.
208. Mendez,A., Smerdou,C., Izeta,A., Gebauer,F. and Enjuanes,L. (1996) Molecular characterization of transmissible gastroenteritis coronavirus defective interfering genomes: packaging and heterogeneity. *Virology*, **217**, 495–507.
209. Zust,R., Miller,T.B., Goebel,S.J., Thiel,V. and Masters,P.S. (2008) Genetic interactions between an essential 3′ cis-acting RNA pseudoknot, replicase gene products, and the extreme 3′ end of the mouse coronavirus genome. *J. Virol.*, **82**, 1214–1228.
210. Hsue,B. and Masters,P.S. (1997) A bulged stem-loop structure in the 3′ untranslated region of the genome of the coronavirus mouse hepatitis virus is essential for replication. *J. Virol.*, **71**, 7567–7578.
211. Goebel,S.J., Hsue,B., Dombrowski,T.F. and Masters,P.S. (2004) Characterization of the RNA components of a putative molecular switch in the 3′ untranslated region of the murine coronavirus genome. *J. Virol.*, **78**, 669–682.
212. Deo,R.C., Bonanno,J.B., Sonenberg,N. and Burley,S.K. (1999) Recognition of polyadenylate RNA by the poly(A)-binding protein. *Cell*, **98**, 835–845.
213. Ozturk,S. and Uysal,F. (2018) Potential roles of the poly(A)-binding proteins in translational regulation during spermatogenesis. *J. Reprod. Dev.*, **64**, 289–296.
214. Smith,R.W., Blee,T.K. and Gray,N.K. (2014) Poly(A)-binding proteins are required for diverse biological processes in metazoans. *Biochem. Soc. Trans.*, **42**, 1229–1237.
215. Villalba,A., Coll,O. and Gebauer,F. (2011) Cytoplasmic polyadenylation and translational control. *Curr. Opin. Genet. Dev.*, **21**, 452–457.
216. Radford,H.E., Meijer,H.A. and de Moor,C.H. (2008) Translational control by cytoplasmic polyadenylation in Xenopus oocytes. *Biochim. Biophys. Acta*, **1779**, 217–229.
217. Hofmann,M.A. and Brian,D.A. (1991) The 5′ end of coronavirus minus-strand RNAs contains a short poly(U) tract. *J. Virol.*, **65**, 6331–6333.
218. Peng,Y.H., Lin,C.H., Lin,C.N., Lo,C.Y., Tsai,T.L. and Wu,H.Y. (2016) Characterization of the Role of Hexamer AGUAAA and Poly(A) Tail in Coronavirus Polyadenylation. *PLoS One*, **11**, e0165077.
219. Wu,H.Y., Ke,T.Y., Liao,W.Y. and Chang,N.Y. (2013) Regulation of coronaviral poly(A) tail length during infection. *PLoS One*, **8**, e70548.
220. Shien,J.H., Su,Y.D. and Wu,H.Y. (2014) Regulation of coronaviral poly(A) tail length during infection is not coronavirus species- or host cell-specific. *Virus Genes*, **49**, 383–392.
221. Tvarogova,J., Madhugiri,R., Bylapudi,G., Ferguson,L.J., Karl,N. and Ziebuhr,J. (2019) Identification and characterization of a human coronavirus 229E nonstructural Protein 8-Associated RNA 3′-Terminal Adenylyltransferase activity. *J. Virol.*, **93**, e00291-19.
222. Spagnolo,J.F. and Hogue,B.G. (2000) Host protein interactions with the 3′ end of bovine coronavirus RNA and the requirement of the poly(A) tail for coronavirus defective genome replication. *J. Virol.*, **74**, 5053–5065.
223. Tsai,T.L., Lin,C.H., Lin,C.N., Lo,C.Y. and Wu,H.Y. (2018) Interplay between the Poly(A) Tail, Poly(A)-Binding protein, and coronavirus nucleocapsid protein regulates gene expression of coronavirus and the host cell. *J. Virol.*, **92**, e01162-18.
224. Brockway,S.M., Clay,C.T., Lu,X.T. and Denison,M.R. (2003) Characterization of the expression, intracellular localization, and replication complex association of the putative mouse hepatitis virus RNA-dependent RNA polymerase. *J. Virol.*, **77**, 10515–10527.
225. Baric,R.S. and Yount,B. (2000) Subgenomic negative-strand RNA function during mouse hepatitis virus infection. *J. Virol.*, **74**, 4039–4046.
226. Sawicki,S.G. and Sawicki,D.L. (1990) Coronavirus transcription: subgenomic mouse hepatitis virus replicative intermediates function in RNA synthesis. *J. Virol.*, **64**, 1050–1056.
227. Sethna,P.B., Hung,S.L. and Brian,D.A. (1989) Coronavirus subgenomic minus-strand RNAs and the potential for mRNA replicons. *PNAS*, **86**, 5626–5630.
228. Zuniga,S., Sola,I., Alonso,S. and Enjuanes,L. (2004) Sequence motifs involved in the regulation of discontinuous coronavirus subgenomic RNA synthesis. *J. Virol.*, **78**, 980–994.
229. Jauregui,A.R., Savalia,D., Lowry,V.K., Farrell,C.M. and Wathelet,M.G. (2013) Identification of residues of SARS-CoV nsp1 that differentially affect inhibition of gene expression and antiviral signaling. *PLoS One*, **8**, e62416.
230. Gomez,G.N., Abrar,F., Dodhia,M.P., Gonzalez,F.G. and Nag,A. (2019) SARS coronavirus protein nsp1 disrupts localization of Nup93 from the nuclear pore complex. *Biochem. Cell. Biol.*, **97**, 758–766.
231. Prentice,E., McAuliffe,J., Lu,X., Subbarao,K. and Denison,M.R. (2004) Identification and characterization of severe acute respiratory syndrome coronavirus replicase proteins. *J. Virol.*, **78**, 9977–9986.
232. GhisolfiNieto,L., Joseph,G., PuvionDutilleul,F., Amalric,F. and Bouvet,P. (1996) Nucleolin is a sequence-specific RNA-binding protein: Characterization of targets on pre-ribosomal RNA. *J. Mol. Biol.*, **260**, 34–53.
233. Boccaletto,P., Machnicka,M.A., Purta,E., Piatkowski,P., Baginski,B., Wirecki,T.K., de Crecy-Lagard,V., Ross,R., Limbach,P.A., Kotter,A. *et al.* (2018) MODOMICS: a database of RNA modification pathways. 2017 update. *Nucleic Acids Res.*, **46**, D303–D307.

234. Zhao,B.X.S., Roundtree,I.A. and He,C. (2017) Post-transcriptional gene regulation by mRNA modifications. *Nat. Rev. Mol. Cell Biol.*, **18**, 31–42.
235. Williams,G.D., Gokhale,N.S. and Horner,S.M. (2019) Regulation of Viral Infection by the RNA Modification N6-Methyladenosine. *Ann. Rev. Virol.*, **6**, 235–253.
236. Chen,J.N., Jin,L., Wang,Z.M., Wang,L.Y., Chen,Q.B., Cui,Y.R. and Liu,G.L. (2020) N6-methyladenosine regulates PEDV replication and host gene expression. *Virology*, **548**, 59–72.
237. Zhou,Y., Zeng,P., Li,Y.H., Zhang,Z.D. and Cui,Q.H. (2016) SRAMP: prediction of mammalian N-6-methyladenosine (m(6)A) sites based on sequence-derived features. *Nucleic Acids Res.*, **44**, e91.